https://doi.org/10.5194/egusphere-2023-157
Preprint. Discussion started: 23 February 2023

Stagnant ice and age modelling in the Dome C region, Antarctica

Ailsa Chung[1], Frédéric Parrenin[1], Daniel Steinhage[2], Robert Mulvaney[3], Carlos Martín[3], Marie G.P. Cavitte[4], David A. Lilien[5,6], Veit Helm[2], Drew Taylor[7], Prasad Gogineni[7], Catherine Ritz[1], Massimo Frezzotti[9], Charles O'Neill[7], Heinrich Miller[2], Dorthe Dahl-Jensen[5,6], and Olaf Eisen[2,8]

[1]Université Grenoble Alpes, CNRS, IRD, IGE, 38000 Grenoble, France
[2]Alfred-Wegener-Institut Helmholz-Zentrum für Polar-und Meeresforschung, Bremerhaven, Germany
[3]British Antarctic Survey, Cambridge, United Kingdom
[4]Earth and Life Institute, Georges Lemaître Centre for Earth and Climate Research, Université catholique de Louvain, Belgium
[5]Physics of Ice, Climate and Earth, Niels Bohr Institute, University of Copenhagen, Copenhagen, Denmark
[6]Centre for Earth Observation Science, University of Manitoba, Winnipeg, Canada
[7]Remote Sensing Center, University of Alabama, Tuscaloosa, AL, USA
[8]Fachbereich Geowissenschaften, Universität Bremen, Bremen, Germany
[9]Department of Science, University Roma Tre, Rome, Italy

Correspondence: Ailsa Chung (ailsa.chung@univ-grenoble-alpes.fr, frederic.parrenin@univ-grenoble-alpes.fr)

Abstract. We present a 1D numerical model which calculates the age of ice around Dome C. It accounts either for melting or for a layer of stagnant ice above the bedrock. It is constrained by horizons picked from radar observations and dated using the EPICA Dome C (EDC) ice core age profile. We used 3 different radar datasets with the widest reaching airborne radar system covering an area of 10,000 km^2 and zooming in to 5 km transects over Little Dome C (LDC) with a ground based system. We find that stagnant ice exists in many places including above the LDC relief where the new Beyond EPICA drill site (BELDC) is located. The modelled thickness of this layer of stagnant ice roughly corresponds to the thickness of the basal unit observed in one of the radar surveys and observations made with Autonomous phase-sensitive Radio-Echo Sounder (ApRES). At BELDC, the modelled stagnant ice thickness is 182±63 m and the modelled maximum age (that we define as the age at a maximum age density of 20 kyr m^{-1}) is 1.49±0.18 Ma at a depth of 2505±34 m. This is very similar to all sites situated on the LDC relief such as that of the Million Year Ice Core project being conducted by the Australian Antarctic Division. The model was also applied to radar data in the area 10-20 km north of EDC (North Patch, NP), where we find either a thin layer of stagnant ice (generally <60 m) or a very low melt rate (<0.1 mm yr^{-1}). The modelled maximum age at NP is over 2 Ma in most places, with ice at 1.5 Ma having a resolution of 9-12 kyr m^{-1} , making it an exciting prospect for a future oldest ice drill site.

https://doi.org/10.5194/egusphere-2023-157
Preprint. Discussion started: 23 February 2023

1 Introduction

The Mid-Pleistocene Transition (MPT) marks the change in climate glacial-interglacial cycles from those with low amplitude and around 41 kyr periodicity to the current high-amplitude cycles of 100 kyr on average (Clark et al., 2006). The MPT took place between 1250 and 700 ka. Understanding the factors that affected past glacial cycles can help us to construct models to predict how human emissions will affect the climate in the future. Ice cores provide unique insights into the climate of the past (EPICA members, 2004). To date, the oldest continuous ice core record extracted from Antarctica is from the EPICA Dome C (EDC) core, which goes back ~ 800 ka (Bazin et al., 2013). The Oldest Ice Challenge defined by the International Partnership in Ice Core Sciences (IPICS) community now aims to study the MPT using an ice archive from Antarctica. A potential site has been defined $\sim$35 km southwest of EDC, near a secondary dome called Little Dome C (LDC). There, the mountainous bedrock is thought to prevent basal melting (Parrenin et al., 2017; Passalacqua et al., 2017; Lilien et al., 2021) and the overall glaciological conditions seem to satisfy the boundary conditions recommended by the IPICS community (Fischer et al., 2013). The European Beyond EPICA project aims to extract a continuous ice core of up to 1.5 Ma, with a maximum age density of 20 kyr m^{-1} at this site called Beyond EPICA Little Dome C (BELDC).

A fundamental question for the Oldest Ice sites on the East Antarctic plateau such as BELDC is; is the deepest ice which lies just above the bedrock useful for paleoclimatic reconstructions? When examining the Vostok ice core, a layer of deformed ice was found just above the bedrock (Souchez et al., 2002). Isotopic analysis showed that the bottom 228 m of the ice core had deformed as a result of folding and intermixing at a submetric scale. At the bottom of the EDC ice core, there is a section of around 60-70 m where the electrochemical properties are very different from those of the shallower ice. Generally known as the basal layer, the mechanics of this deformed ice are not well understood. While its isotopic composition has been studied (Tison et al., 2015), the interpretation of these results remains uncertain. The mechanical stress on the deepest ice has distorted the timescale and left no clear paleoclimatic record. Basal ice was difficult to observe using previous radar systems due to the presence of the formerly called echo-free zone (EFZ) and the related change in the dielectric properties at this depth could be due to folding, buckling, recirculation, recrystallisation or sharp thermal transition (Drews et al., 2009). The EFZ is a band just above the bed and hundreds of meters thick, where there are no observed layers in radargrams. However, during the analysis of the EPICA Dronning Maud Land ice core (EDML), Ruth et al. (2007) found stratigraphically conserved ice at EDML in the upper 50% of the EFZ. Therefore, even with the absence of visible layers in the radargram, there can still be a detectable paleoclimatic signal in the ice.

In their modeling work, Parrenin et al. (2007) used the ice-bedrock interface as the bottom boundary condition. But given the smoothness of the basal isochrones compared to the roughness of the observed ice-bedrock interface, it was suggested that a layer of stagnant ice could exist above some areas of the bedrock (Parrenin et al., 2007, 2017). More recently, a basal layer of ice with different dielectric properties, called the “basal unit”, has been documented in radar imaging. Lilien et al. (2021) found that at the Beyond EPICA drill site on Little Dome C in Antarctica, the basal unit is around 200 m thick. They found that at this depth there was a change in return power and lateral coherency of the signals which is likely to come from a change in the physical properties of the ice. This is in contrast to the EFZ which seems to be caused by a backscatter power that is too

https://doi.org/10.5194/egusphere-2023-157
Preprint. Discussion started: 23 February 2023

low, below the noise level, and therefore cannot not be imaged (Drews et al., 2009). Lilien et al. (2021) also modelled the age depth profile at the BELDC drill site, inverting the optimal value of the thickness of a layer of stagnant ice, which was found to be close to the observed thickness of the basal unit. However, Lilien et al. (2021) only applied this 1D model in one place, the BELDC site. Modelling over the whole Dome C region would give a better idea of the spatial extent of this potentially stagnant ice layer, its role in the overall ice-dynamic behaviour and other potential Oldest Ice drilling sites. This is the objective of this study.

Here, we present a 1D numerical model which uses inverse methods to infer a layer of stagnant ice from the isochronal information. This model is applied to three radar datasets acquired in recent years which cover the larger Dome C area. We then compare the thickness of the modelled stagnant ice with the basal unit observed in the radar, and propose that they are one and the same. We further corroborate this hypothesis using measurements made with Autonomous phase-sensitive Radio-Echo Sounder (ApRES), which show that the vertical velocity profile at LDC is better described when there is a layer of stagnant ice above the bedrock. We discuss the expectations for the Beyond EPICA ice core based on our modelling results and also take a closer look at an area 10-20 km north of EDC, known as North Patch (NP), which could be an interesting site for a future Oldest Ice drilling projects.

2 Numerical age model

2.1 Method summary

We use a modified version of the Parrenin et al. (2017) 1D numerical age model. The model is applicable to areas centered on domes or near ice divides where there is little to no horizontal ice flow and the bedrock relief is relatively smooth. It is based on the pseudo-steady assumption which means that the geometry and vertical velocity profile are steady. The only temporal variation is related to accumulation and derived from the EDC ice core reconstruction (Bazin et al., 2013). The modifications we apply to the Parrenin et al. (2017) model relate to the thermal representation. While Parrenin et al. (2017) include an explicit temperature scheme, accounting for the geothermal flux, we use a simpler approach which allows for stagnant ice above the bedrock. We do so by using a *mechanical ice thickness* H_m which is different to the observed ice thickness H_{obs} (Fig. 1). We also assume that there is no melting at H_m. $H_m < H_{obs}$ (stagnant ice case) means there is a layer of stagnant ice of thickness $H_{obs} - H_m$, and the age goes to infinity at depth H_m. $H_m > H_{obs}$ (melting case) means that there is some melting at H_{obs} which is calculated by the truncation of the vertical velocity profile at H_{obs}. In this case, the age profile is truncated to H_{obs} meaning that the age at H_{obs} is finite.

https://doi.org/10.5194/egusphere-2023-157
Preprint. Discussion started: 23 February 2023

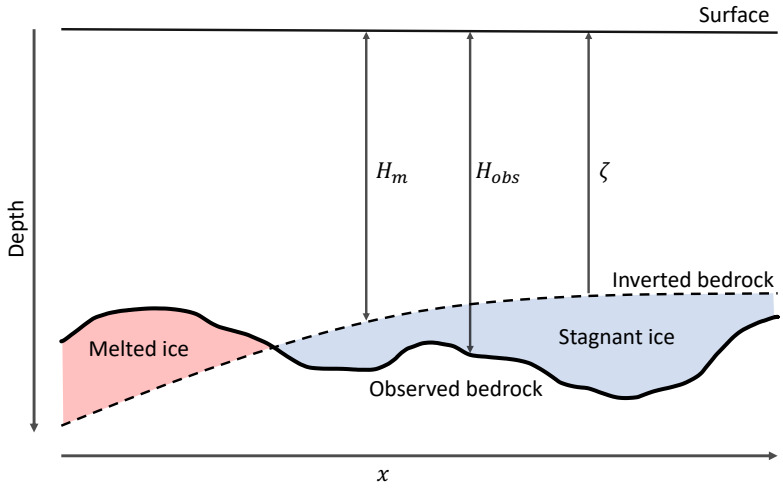

Figure 1. Diagram showing mechanical ice thickness H_m and radar observed ice thickness H_{obs}. The melted ice case is in red and stagnant ice case is in blue. The normalised ice elevation ζ is 0 at the inverted bedrock H_m and 1 at the surface.

2.2 Forward model

As in Parrenin et al. (2017), we compute the true age from a so-called steady age using the change of time variable

$$\bar{t} = \int_0^t r(t')dt', \tag{1}$$

where $r(t)$ is the ratio of the EDC accumulation rate (Bazin et al., 2013) to its temporally averaged value. Beyond the extent of the EDC record (800 ka), we assume $r(t) = 1$.

The steady-age of the ice ($\bar{\chi}$) at a given spatial position x is

$$\bar{\chi}(\zeta) = \int \frac{H_m}{\bar{a}\tau(\zeta)} d\zeta, \tag{2}$$

where $\bar{a}$ is the average accumulation rate and ζ is the normalized vertical coordinate (0 at H_m, 1 at the surface).

Since there is no melting at H_m, the thinning function τ is equal to the horizontal flux shape function ω. Here we use the Lliboutry velocity profile (Lliboutry, 1979),

$$\tau(\zeta) = \omega(\zeta) = 1 - \frac{p+2}{p+1}(1-\zeta) + \frac{1}{p+1}(1-\zeta)^{p+2}, \tag{3}$$

where the parameter p modifies the non-linearity of ω (with larger p, ω becomes more linear). In the melting case, the basal melt rate is calculated by $m = \bar{a}\omega(H_{obs}/H_m)$

https://doi.org/10.5194/egusphere-2023-157
Preprint. Discussion started: 23 February 2023

2.3 Optimisation

For this model, we use the Scipy least squares optimisation with the Trust Region Reflective algorithm. It gives an optimised value for inverted parameters and a covariance matrix from which we derive an uncertainty for each parameter. To prevent $p < -1$ and $H_m < 0$, we implement the scheme using $p = e^{p'} - 1$, also done in Parrenin et al. (2017), and $H_m = e^{H'_m}$. The three inverted parameters are the surface accumulation rate $\bar{a}$, the Lliboutry profile parameter p' and log of the ice thickness H'_m. The minimised cost function uses the least-squares expression:

$$S = \sum \frac{\left(\chi_i^{iso} - \chi^{mod}\left(d_i^{iso}\right)\right)^2}{\left(\sigma_i^{iso}\right)^2} + \frac{\left(p'_{prior} - p'\right)^2}{\left(\sigma^{p'}\right)^2}, \tag{4}$$

where $p'_{prior} = 3$, a similar value to EDC and $\sigma^{p'} = 1$, to allow the function to vary within reasonable limits.

Isochrones which have been traced and dated from radar observations, constrain the optimisation in the model. In order to assess the suitability of the model in representing the observed isochrones at each spatial position, we calculate the standard deviation of the residuals between observed isochrone ages and modelled ages,

$$\sigma_R = \sqrt{\frac{R^T R}{n_{iso}}}, \quad R = \frac{(\bar{\chi}_{iso}) - (\bar{\chi}_{mod})}{\bar{\sigma}_{iso}} \tag{5}$$

where R is a vector of the residuals and n_{iso} is the number of isochrones. If the model is a good fit, then σ_R is close to 0. However, if $\sigma_R > 2$, it means the model is not an accurate representation of the observations. This often occurs in areas such as the flank of the dome or over trenches in the bedrock where horizontal ice flow is an important factor.

3 Datasets

In this study we make use of three radar surveys collected in the LDC region, which were taken in almost consecutive Antarctic field seasons and informed the selection of the location of the Beyond EPICA drill site (BELDC). As three different radar systems were used, we treat each dataset independently and compare the model results obtained. We focus on three different scales which correspond to the differing spatial coverages of the three surveys over LDC. We also look at the NP site which was investigated in one of the surveys and was initially tagged as a site of interest for Oldest Ice (Fig. 2). In Fig. 2, we mark BELDC (75.29917° S, 122.44516° E) and the site selected for the Million Year Ice Core project drilling (MYIC; 75.34132° S, 122.52059° E).

Internal reflecting horizons (IRH) were traced in each of the datasets in the two-way travel time domain. The depths of these IRHs were then calculated using the electromagnetic wave velocity in ice 168.5 m μs^{-1} (Winter et al., 2017) and a firn correction of 10 m with an uncertainty of ± 3 m (Lilien et al., 2021). In this section, we also briefly describe an Autonomous phase-sensitive Radio-Echo Sounder (ApRES) used to determine the vertical velocity of the ice at two selected locations, at EDC and near BELDC.

https://doi.org/10.5194/egusphere-2023-157
Preprint. Discussion started: 23 February 2023

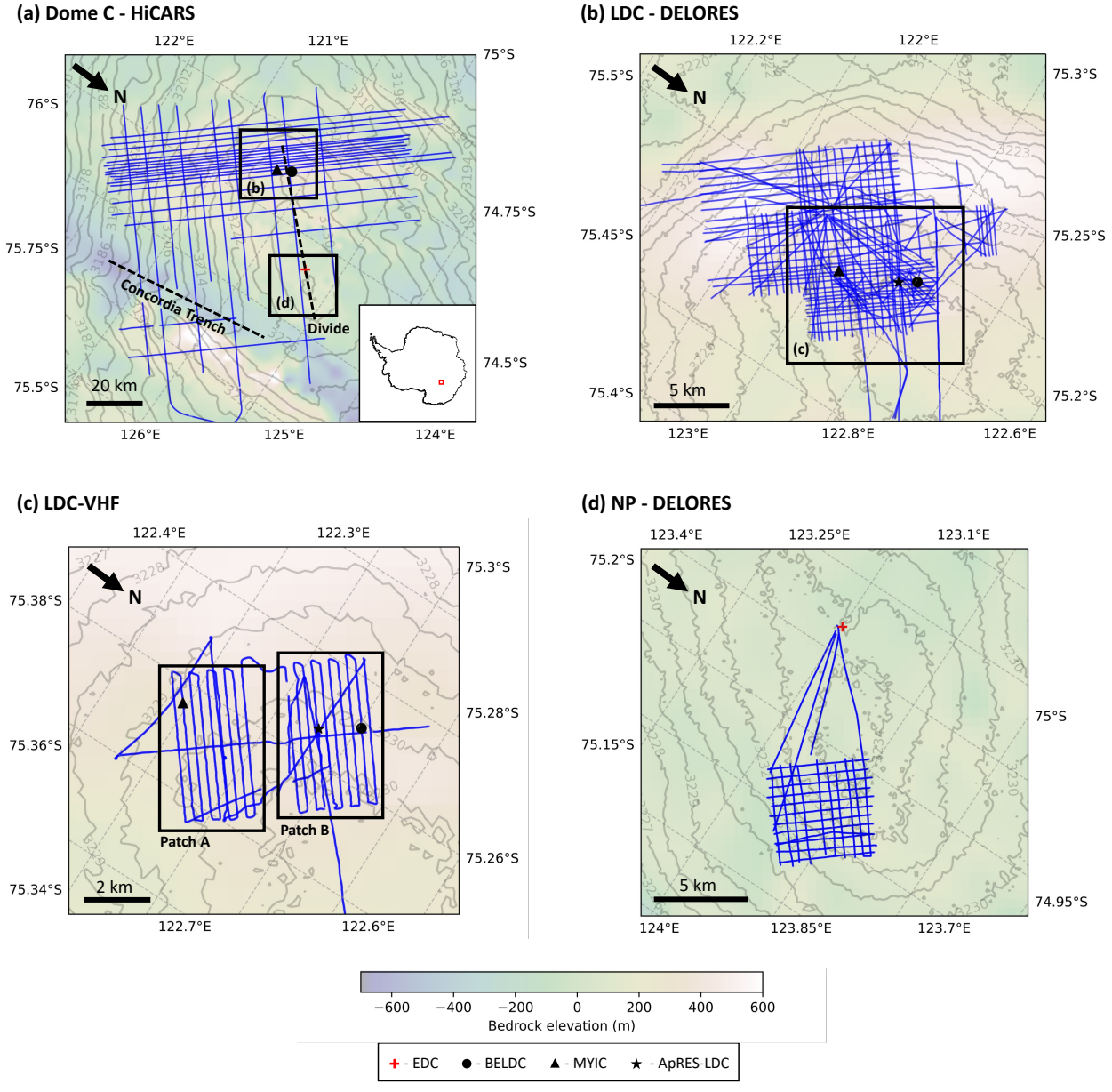

Figure 2. Maps showing the four areas of interest near Dome C with bedrock elevation from Bedmachine version 3 (Morlighem, 2022) and surface elevation from REMA (Howat et al., 2019). Radar transects of each survey are in blue. Ice core drill sites EDC, BELDC, MYIC and the ApRES-LDC site are marked by a red cross, black circle, black triangle and black star respectively. **(a)** The larger Dome C region covered by the HiCARS airborne radar transects. The black dashed lines show the Concordia trench and Dome C divide. In the inset, the red square shows the location of Dome C in Antarctica. **(b)** LDC DELORES ground based radar dataset, **(c)** LDC-VHF high resolution ground based radar dataset,**(d)** NP DELORES dataset.

https://doi.org/10.5194/egusphere-2023-157
Preprint. Discussion started: 23 February 2023

3.1 UTIG HiCARS

The Oldest Ice candidate A (OIA) survey was conducted in January 2016 by the University of Texas at Austin Institute for Geophysics (UTIG), the Australian Antarctic Division (AAD) and the French Polar Institute Paul-Émile Victor (IPEV) as part of the ICECAP project (International Collaborative Exploration of the Cryosphere through Airborne Profiling, Cavitte et al., 2016). Data were collected with the High Capability Airborne Radar Sounder (HiCARS) 1 and 2, operating over frequency range 52.5–67.5 MHz (Cavitte et al., 2021), and were processed and published in Young et al. (2017); Cavitte et al. (2020, 2021). These data cover an area around 100×100 km^2 over LDC and intersect the EDC site for dating. Twenty-six IRHs were traced and nineteen of those could be dated at the EDC site (Table 3 of Cavitte et al., 2021, provides IRH ages and uncertainties). The IRH depths range from 308.2±3.2 m to 2644±12 m and ages range from 10.0±0.3 ka to 366.5±7.9 ka. In this study, we use the 19 dated IRHs which we re-interpolate spatially to a point every 100 m for input into the 1D model, in order to get a result of reasonable resolution while optimising computation time.

3.2 BAS DELORES

Over the Antarctic field seasons 2016–17 and 2017–18, the sledge-borne DEep LOoking Radio Echo Sounder (DELORES) from the British Antarctic Survey (BAS) was used to explore two potential drill sites around the Dome C area, identified from the HiCARS survey results. The LDC area is covered by a dense network of 120 radar transects, mostly organised as a grid, with denser spots in areas of particular interest. DELORES is the only radar system to survey NP at high spatial resolution, collecting a grid of 21 radar transects, covering an area of approximately 5×5 km^2. We discuss the LDC and NP areas separately, but it should be noted that the same 20 IRHs were traced manually over all DELORES radar lines. For the model, we re-interpolate the horizontal spacing to 10 m.

In order to date the IRHs, LDC is linked to the EDC ice core site through three independent radar transects, while NP is linked through one transect to EDC. Ages for IRHs were then calculated by linearly interpolating the EDC age-depth timescale from AICC2012 (Bazin et al., 2013) where the IRHs are closest to the ice core site. As the depth difference between values in the AICC2012 dataset is 1.55 m, there is no need for more complex interpolation as the uncertainty is negligible relative to other factors. The age of each IRH is obtained by first calculating the average of the ages obtained from the three EDC–LDC radar intersections, and then averaging with the EDC–NP intersection. It is this average age of each IRH that is input to the model.

The depth uncertainty arises from several contributions. The DELORES radar system operating over frequency range 0.6–7 MHz has a vertical resolution of 11.1 m and range precision of 3 m (Cavitte et al., 2021). The two-way travel time to depth conversion results in a firn correction uncertainty of ±3 m (Lilien et al., 2021) and ±0.44% uncertainty for the wave speed in ice. The final source of depth uncertainty is due to the slope of the isochrones and the distance between the EDC site and the point of closest approach of each of the four radar transects used for dating (338–404 m). The gradient of each IRH over the last traceable 100 m is extrapolated over this gap, resulting in an uncertainty contribution of 1 to 15 m, increasing with depth. Combining the various sources of uncertainties gives an overall depth uncertainty of 12 m for the shallowest IRH to

https://doi.org/10.5194/egusphere-2023-157
Preprint. Discussion started: 23 February 2023

23 m for the deepest IRH. The calculated ages for each horizon are in Table I along with uncertainties which take into account that of the depth and of the AICC2012 age-depth profile (Bazin et al., 2013).

3.3 UA LDC-VHF

In the 2019/20 Antarctic field season, a multichannel coherent depth sounder operating in the VHF frequency range was deployed to survey the potential Beyond EPICA drill sites in the LDC area, known as Patch A and Patch B (Fig. 2c, Yan et al., 2020; Lilien et al., 2021). Due to logistical and time constraints, a polarimetric ultra-wideband system operating over 170-470 MHz and a new ultra-high frequency system operating at 600-900 MHz with a large array in a Mills Cross array configuration could not be deployed. Those systems were developed by The University of Alabama (UA), the University of Copenhagen (CPH) and the Alfred Wegener Institute (AWI). UA also developed a high-power radar operating at 200 MHz with 60 MHz bandwidth to complement and supplement data from the other radars, and this system was used in 2019/20. It was capable of transmitting 8 µs chirped pulses with 500 W peak power per channel at a pulse repetition frequency of 10 kHz (Yan et al., 2020). This system was operated with much reduced sensitivity because of the the failure of the balloon carrying the antenna structure and the compact power generator housed close to the radar system. The generator failure led to a large secondary generator being mounted on a metal structure between the vehicle and the antenna arrays. A long power cable powered the system in the tracked vehicle, and radio-frequency cables were forced to route next to the generator. These complications forced the field team to reduce the peak power to less than 100 W for each channel and operate only four channels to reduce radio-frequency interference (RFI) issues. In the following, we will refer to data collected using this system as the LDC-VHF radar dataset. The dataset consists of 12 transects systematically covering Patches A and B with parallel lines. In this study, we traced 19 IRHs along the 12 radar transects and re-interpolated to a 10 m horizontal spacing. A delay time of 1 µs was required during processing, and was confirmed by matching the reflectivity pattern and bedrock reflection at the EDC end of the profile to those of the radar data presented in (Winter et al., 2017). The IRHs were then dated using the direct radar transect link from LDC to the EDC ice core site. These IRHs and bedrock reflections were traced and dated independently of Lilien et al. (2021), who focused only on the EDC–LDC transect.

There are two components which make up the isochrone age uncertainty. The first comes from the dating of the EDC ice core in AICC2012 (Bazin et al., 2013, Table 2). The second component, the depth uncertainty, is determined using the method in Lilien et al. (2021), who also used this radar data. It includes three factors: 3 m firn depth uncertainty; 1% dielectric constant uncertainty; and the gradient uncertainty over the 178 m gap from the transect to EDC (1 to 6 m). The overall depth uncertainty ranged from 11 to 33 m from the shallowest to the deepest IRH. The calculated ages and uncertainties are shown in Table II.

The high vertical resolution of the radar data shows a layer of ice just above the bedrock where there is an abrupt change in the return power and lateral coherency of the radar signal. In this layer, there are no visible continuous IRHs, although the radar system is effective at these depths, as the signal-to-noise ratio is sufficiently high to detect continuous IRHs. This layer was first presented in Lilien et al. (2021) and termed the basal unit. It is also visible in other datasets with varying clarity (e.g., Winter et al., 2017), but in particular also in the HiCARS data (Cavitte, 2017). In this study, we traced the depth of the top of the basal unit where it was visible in the radargrams.

https://doi.org/10.5194/egusphere-2023-157
Preprint. Discussion started: 23 February 2023

DELORES IRHs	Depth at EDC (m)	Age (ka)	Age uncertainty (ka)
	H	χ	σ_χ
IRH_1	317	10.5	0.5
IRH_2	606	30.4	1.5
IRH_3	705	39.2	1.1
IRH_4	798	47.1	1.4
IRH_5	961	62.2	2.4
IRH_6	1084	75.2	2.2
IRH_7	1136	80.0	1.9
IRH_8	1169	82.6	1.9
IRH_9	1339	97.7	2.1
IRH_10	1454	108.3	2.5
IRH_11	1682	128.5	2.0
IRH_12	1903	166.1	4.7
IRH_13	2077	202.3	3.5
IRH_14	2263	240.4	3.8
IRH_15	2344	262.2	6.9
IRH_16	2526	326.2	6.6
IRH_17	2592	345.5	10.1
IRH_18	2659	381.5	12.3
IRH_19	2687	395.8	10.0
IRH_20	2740	414.6	10.5
Bedrock	3198	-	-

Table I. IRHs traced in the DELORES radar dataset, average depth at EDC, calculated average age and uncertainty.

3.4 BAS/UCL ApRES

185 During the 2016–17 and 2017–18 field seasons, the Autonomous phase-sensitive Radio-Echo Sounder (ApRES) was also used in two locations to explore englacial flow. Nicholls et al. (2015) give an overview of the system, data processing workflow and applications that we simply summarize here for convenience.

ApRES is a ground-based radar system capable of tracking temporal displacement in the position of IRHs. The position changes are transformed from travel-time to depth following Kingslake et al. (2016) using the density from EDC (Le Meur
190 et al., 2018). Due to the particularities of basal ice in the area, ApRES was capable of detecting reflectivity events as close as 20 m from the bed in the two successive field seasons. These events were used as a reference to transform IRH vertical displacement into full-depth vertical velocity. ApRES measurements were taken at EDC and at a location at LDC, Patch B near BELDC (ApRES-LDC, star in Fig. 2, 75.30832 °S,122.46902 °E).

https://doi.org/10.5194/egusphere-2023-157
Preprint. Discussion started: 23 February 2023

IRH no.	Depth at EDC (m)	Age (ka)	Age uncertainty (ka)
	H	χ	σ_χ
IRH_1	1079	73.7	2.4
IRH_2	1206	84.6	2.1
IRH_3	1270	90.3	2.2
IRH_4	1342	96.9	2.3
IRH_5	1507	113.5	2.6
IRH_6	1596	121.3	2.2
IRH_7	1747	132.9	3.1
IRH_8	1889	160.5	5.7
IRH_9	1977	180.1	5.5
IRH_10	2095	203.1	4.7
IRH_11	2165	215.2	4.5
IRH_12	2274	240.2	5.2
IRH_13	2296	243.7	5.3
IRH_14	2486	304.9	10.8
IRH_15	2525	321.2	10.2
IRH_16	2584	337.0	9.9
IRH_17	2646	367.4	16.2
IRH_18	2706	397.8	12.8
IRH_19	2826	476.4	26.9
Bedrock	3239	-	-

Table II. IRHs traced in LDC-VHF dataset, depths at EDC, calculated ages and uncertainties.

https://doi.org/10.5194/egusphere-2023-157
Preprint. Discussion started: 23 February 2023

4 Results

4.1 Inferred ages for EDC

In order to evaluate the accuracy of the model, we look at the modelled results for EDC so they can be compared to observations from the ice core. There were three radar transects in the LDC DELORES dataset, one transect in the NP DELORES data and one transect in the LDC-VHF radar dataset which pass close to the EDC drill site. Table III shows the model age result at the points of closest approach to EDC for each radar transect.

	DELORES				LDC-VHF
	DC-LDCRAID2	DC_LDCRAID	DC_LDC_DIVIDE	DC_PNV09B	20201012
distance of closest point to EDC (m)	368	338	338	404	178
total ice thickness (m)	3239	3214	3200	3141	3239
Age at 3189 m depth (ka)	1015±87	1013±86	1016±86	1016±86	971±101

Table III. Modelled results for different radar transects at the points of closest approach to EDC

The three LDC DELORES transects all start at approximately the same point, ∼338–368 m southeast of EDC whereas the NP DELORES transect begins 404 m northeast of EDC. This difference can explain why the total ice thickness is 3141 m for the NP transect but ranges from 3200–3239 m for the LDC transects. The closest point to EDC in the LDC-VHF dataset is 178 m away with an ice thickness of 3239 m. The deepest ice which could be dated in the EDC ice core was at 3189 m depth, where the age inferred from the climatic signals is 801±96 ka (Bazin et al., 2013). At this depth, the modelled ages range from 1013±86 ka to 1016±86 ka for the DELORES dataset and found to be 971±101 ka for the LDC-VHF dataset.

4.2 Stagnant ice and melting

In Fig. 3, we show the results of the stagnant ice thickness or basal melt rate for the four areas of interest. At LDC, the stagnant ice thickness reaches up to ∼250 m and the basal melt rate goes up to ∼3 mm yr^{-1}. From the HiCARS dataset (Fig. 3a), we see that the model predicts a layer of stagnant ice on the LDC bedrock relief. There is significant melting predicted around the edges of the LDC relief, especially on the western side of LDC and across the Concordia trench (Fig. 2a). These areas could also be subject to horizontal flow, implying that the 1D assumption would not be valid in that case. There is a low melt rate on the plateau around EDC which agrees with the findings of the EPICA drill project (EPICA members, 2004; Parrenin et al., 2007; Tison et al., 2015; Passalacqua et al., 2017).

In Figs. 3b and c, we zoom into the LDC area. The DELORES and LDC-VHF radar datasets confirm that there is stagnant ice in this region. Both datasets show stagnant ice thicknesses up to ∼250 m. The DELORES dataset shows that the stagnant ice layer thins to near 0 m at the edge of the LDC relief, but the LDC-VHF dataset shows that near the oldest ice sites at Patch A and Patch B (BELDC and MYIC), the minimum thickness of the stagnant layer remains around 100 m.

https://doi.org/10.5194/egusphere-2023-157
Preprint. Discussion started: 23 February 2023

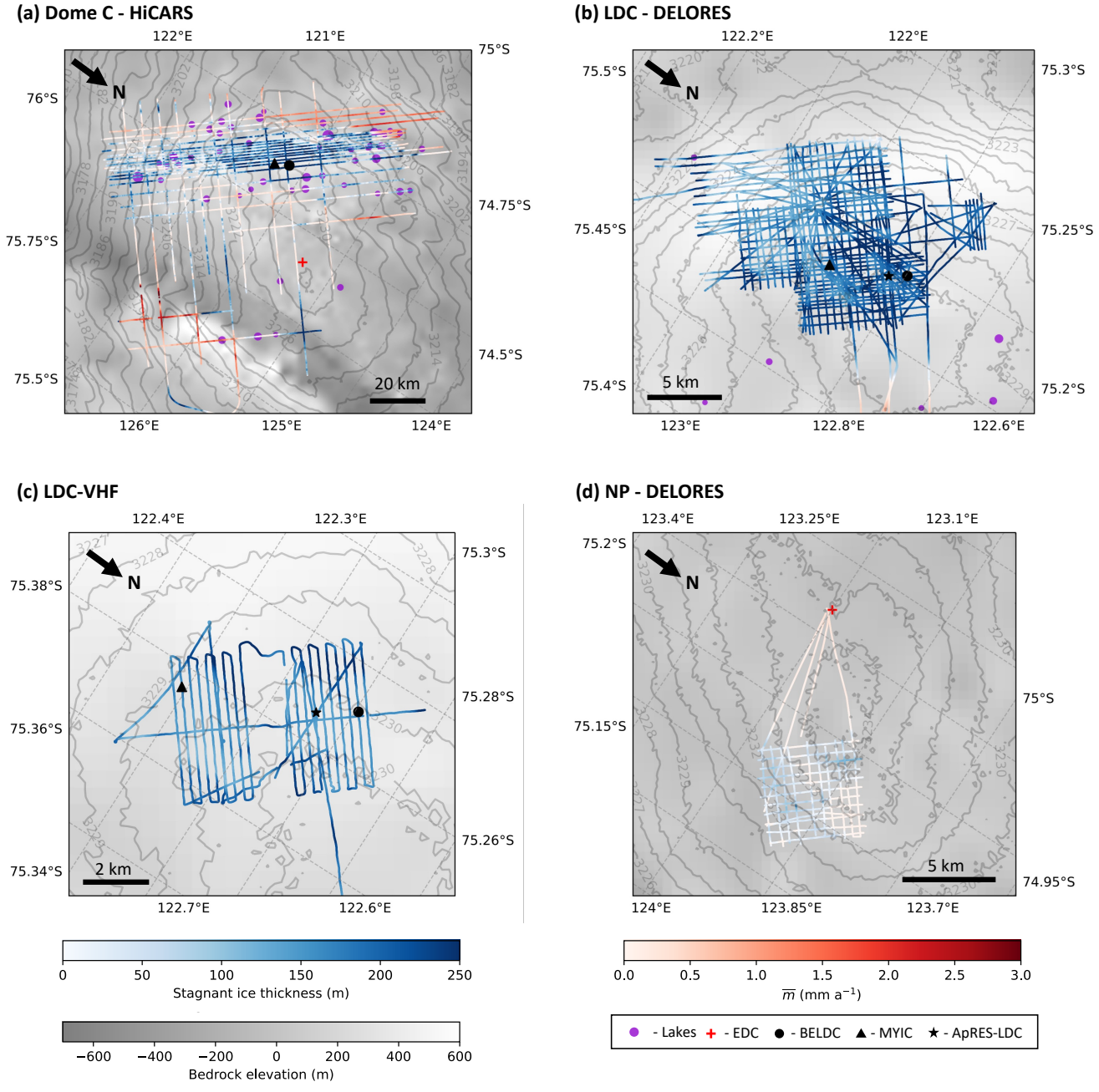

Figure 3. Modelled stagnant ice and basal melting results for each dataset, with panels showing the same areas as in Fig. 2. Stagnant ice thickness, melt rate and bedrock elevation colour bars are the same for all four maps. Lakes are displayed as purple dots (Livingstone et al., 2022). **(a)** HiCARS airborne dataset, **(b)** LDC DELORES ground based radar, **(c)** LDC-VHF high resolution ground based radar dataset, **(d)** NP DELORES dataset.

https://doi.org/10.5194/egusphere-2023-157
Preprint. Discussion started: 23 February 2023

In contrast to LDC, at NP, the mechanical thickness H_m obtained from the model is remarkably similar to the observed bedrock depth from the radar H_{obs}, indicating a lack of melting or stagnant ice (Fig. 3d). There is an area of stagnant ice on the east side of NP but its thickness is generally below 60 m. Where melting occurs, the values are below 0.1 mm yr^{-1}. This low rate is not significant relative to its uncertainty.

4.3 Distribution of the basal unit—indications of stagnant ice

Although features comparable to what we now refer to as the basal unit are visible in many radar datasets over Antarctica (often referred to as echo-free zone, e.g. Drews et al., 2009), the only discussion of the basal unit in our region of interest has so far come from the LDC-VHF radar survey (Lilien et al., 2021). Figure 4a shows the depth of the top of the basal unit traced. Generally, the top of the basal unit is deeper towards the northeast and EDC. This is in large part due to the dip in the local bedrock topography and therefore an increase in ice sheet thickness. In these places, the thickness of the basal unit remains fairly constant, therefore the increase in overall ice sheet thickness results in the increase in depth of the top of the basal unit. There are a couple of anomalous points which do not seem to follow this trend. These come from a mixture of an unclear radar signal and the ambiguity in tracing the basal unit. In contrast, the stagnant ice is a manifestation of the model when the total ice thickness is allowed to vary as the model minimizes the misfit between the observed and modelled isochrones. Figure 4b

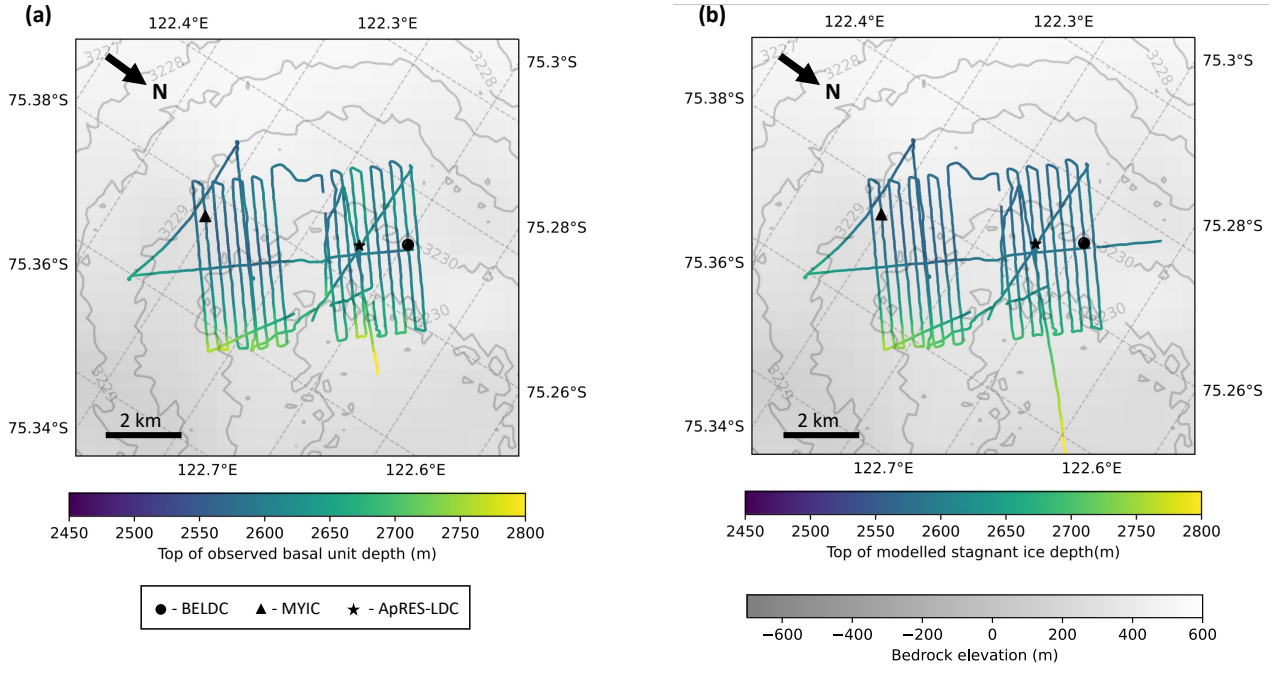

Figure 4. **(a)** Depth of the top of the basal unit traced in the LDC-VHF radar dataset, **(b)** depth of the top of modelled stagnant ice.

https://doi.org/10.5194/egusphere-2023-157
Preprint. Discussion started: 23 February 2023

displays the depth of the top of the modelled stagnant ice. This depth is also equal to the mechanical ice thickness H_m (Fig. 1). It follows the same trend as the basal unit with the deeper values occurring where the bedrock is also deeper.

Comparing Figs. 4a and b, it is clear that the depths of the observed basal unit and the top of the modelled stagnant ice are very similar. Figure 5a shows the model output of a single radar transect in the LDC-VHF dataset. From this, we can see that although the stagnant ice depth does not exactly match that of the observed basal unit, there is a remarkably close relationship between them, given that these values were modelled and observed independently. Overall, the difference between the modelled stagnant ice and observed basal unit thickness generally varies $\pm$60 m (Fig. 5b), with a standard deviation of $\pm$20 m. This corresponds to a difference of approximately 2% relative to the total ice thickness with a standard deviation of $<$1%. The locations with larger differences correspond to the outliers in the basal unit tracing. We should note here that tracing the top of the basal unit in the LDC-VHF radar dataset is ambiguous due to the diffuse nature of the boundary between coherent and incoherent radar returns; different manual interpretations of where this top boundary is can differ by tens of meters.

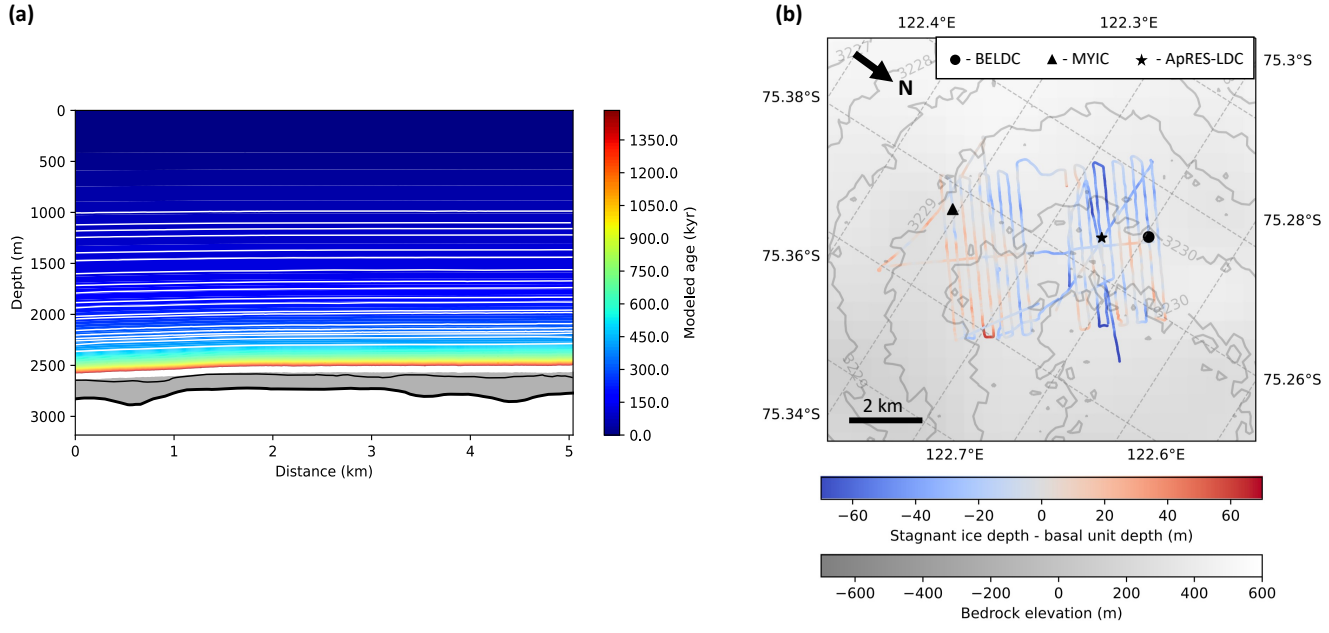

Figure 5. **(a)** A radar transect in the LDC-VHF dataset. The colour gradient shows modelled age corresponding to the side colour bar. The horizontal white lines represent the isochrones traced in the radar data, which constrain the model. Bold black line is bedrock, grey area is modelled stagnant ice layer, and the thin black line is the top of the observed basal unit. All points along the radar transect are categorised as reliable according to Eq. 5. **(b)** Depth of modelled top of stagnant ice minus depth of top of the basal unit, as observed in radar data.

Our model shows that the age distribution of the ice in the LDC area, as described by its isochrones, is better explained when an extensive stagnant basal layer is present. In addition, ApRES measurements offer a glimpse into the internal ice deformation. The ApRES-derived full-depth vertical velocity at the ApRES-LDC site, is shown in Fig. 6a. For reference, we show the englacial vertical velocity at EDC (Fig. 6b) derived previously also using ApRES and presented in Buizert et al.

https://doi.org/10.5194/egusphere-2023-157
Preprint. Discussion started: 23 February 2023

(2021). For the two sites, the best fit Lliboutry velocity profile (Eq. 3) was determined using the ordinary least squares method. For comparison, we also show the vertical velocity profile determined according to the 1D model for the closest points in the DELORES and LDC-VHF datasets. The vertical velocities include not only ice vertical compaction and compression, but also surface thinning/thickening and the vertical component of the along-surface advection. As the 1D model and ApRES data integrate over different time spans, we compare the shape functions that, in the limit of isothermal ice, do not depend on those processes which change with time. We normalise the vertical velocities to the value at 150 m which is below the depth of firn compaction. We can see from the comparisons that the model fits the observations well at both ApRES sites.

Figure 6 shows near surface compaction and almost uniform vertical strain-rate until almost 2000 m depth for ApRES-LDC and a few hundred meters deeper for EDC. At those depths, we are unable to track englacial reflections. This is expected as the radar signal coherence generally deteriorates with depth. However, near the bed, at around 160 m above the bed for ApRES-LDC and about 20 m for EDC, we can track a few strong reflections. The presence of stagnant ice is revealed in ApRES data from two observations. First, for the ApRES-LDC site, the vertical velocity increases rapidly to near zero in the top 2000 m of ice thickness. In this part of the ice column, we have a high density of ApRES data points and our uncertainty is smaller than

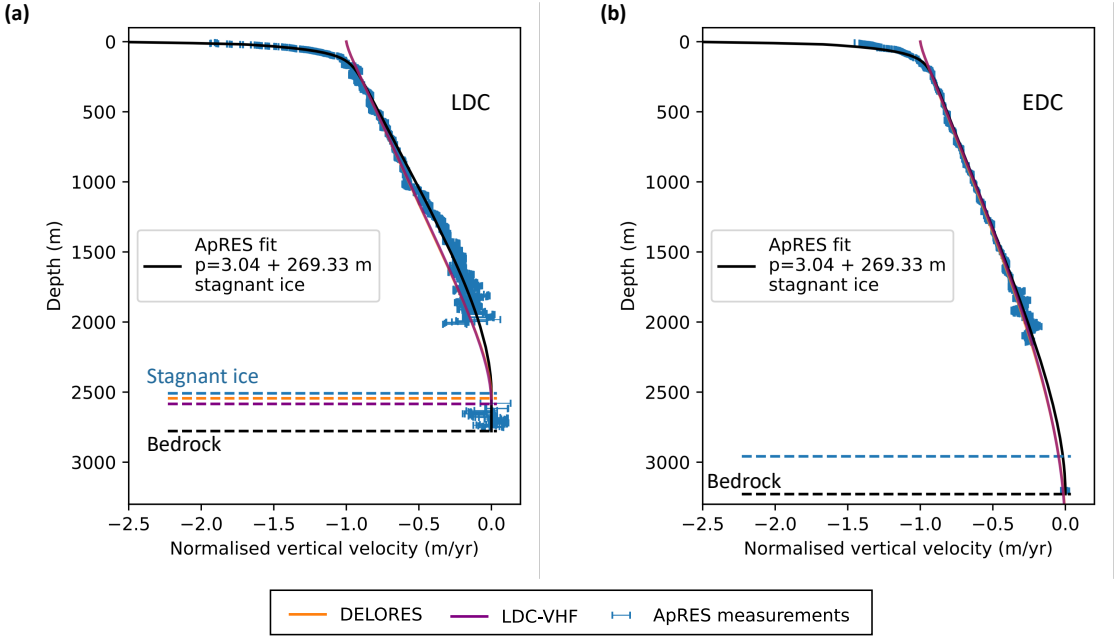

Figure 6. Full-depth vertical velocity derived with ApRES in the proximity of (a) ApRES-LDC at Patch B near BELDC, and (b) EDC. The best fit of the Lliboutry (1979) velocity profile (Eq. 3) to the ApRES data is shown in black. The parameters for the ApRES best fits are: a) for ApRES-LDC $p = 3.04$ with 269.33 m of basal stagnant ice, shown as a dashed blue line, and b) for EDC $p = 3.6$ with no stagnant ice. Orange and purple lines correspond to the vertical velocity fits produced by the 1D model applied to the DELORES and LDC-VHF radar datasets respectively. As the model results are similar for both datasets, the lines are almost entirely superimposed.

https://doi.org/10.5194/egusphere-2023-157
Preprint. Discussion started: 23 February 2023

at the EDC site. If we assume that the absolute value of vertical velocity is decreasing monotonically with depth, it follows that vertical velocity in the bottom section of the column must be smaller than at the EDC, and ice towards the base must be nearly or totally stagnant. Secondly, in the bottom-most hundred meters or so at the ApRES-LDC site, despite the larger uncertainties in the vertical velocity, the simplest explanation for the near-vertical constant vertical strain-rate is that the ice is locally stagnant ice.

4.4 Accumulation rate and p parameter

In Fig. 7, we show the modelled temporally averaged ice-equivalent accumulation rate for each area considered. At LDC, we can see that the accumulation rate is generally around 19 mm yr^{-1}. Looking at Fig 7a, the HiCARS dataset shows that the accumulation rate is higher in surface depressions (red dashed circles) than in the surrounding areas. This is likely because snow is blown into the depressions from areas with higher surface elevation (Cavitte et al., 2018). The accumulation at NP (Fig. 7d) is around 20 mm yr^{-1}, slightly higher than at LDC.

Figure 8 shows how the Lliboutry profile p parameter (Eq. 3) varies across the four surface areas surveyed by the radar systems. The p parameter is quite high at LDC, with values between 5 and 8. Around the edges of LDC, Fig. 8a shows that $p > 8$. At NP (Fig. 8d), where there is little to no modelled stagnant ice, p is much lower, between 2.2 and 3.6.

4.5 Oldest Ice site prospects around Dome C

Two deep ice core drilling campaigns are currently ongoing around the LDC area so we focus on the age modelling results at the two sites. We define the maximum age as the age where the age density is sufficient for paleoclimatic reconstructions with the measurement sensitivities currently achievable, set at 20 kyr m^{-1} (Fischer et al., 2013; Van Liefferinge and Pattyn, 2013). At locations where there is basal melting, the maximum age is the age at the depth of the observed bedrock H_{obs}. Figure 6 shows the maximum age for each of the radar datasets around Dome C. Over the LDC bedrock relief, the maximum age is spatially homogeneous with values around 1.5 Ma. Around the southern and western edges of the LDC relief where melting was predicted (Fig. 3a), the age is much younger, $\sim$0.9-1 Ma. The maximum age is also much younger across the divide from EDC to LDC and over the Concordia trench (Fig 2a).

As the 1.5 Ma ice is on the boundary of the 20 kyr m^{-1} target, we plot age density at 1.2 Ma. Age density is defined as the number of annual layers per meter in the ice column with units of kyr m^{-1}. Figure 10a shows that the age density is generally low around the edges of Dome C, where there is a large amount of melting. Over the LDC relief, where there is stagnant ice, Figs. 10b and c show that the age density for 1.2 Ma ice is 10-14 kyr m^{-1}. Figure 9d shows that the maximum modelled age over the whole radar grid which covers North Patch is around 2 Ma. There is a small area in the north corner of the grid where there is a local bump in the bedrock, therefore the bottom age is slightly younger than where it is smoother. Figure 10d shows that the age density of ice at 1.2 Ma is generally between 5 and 8 kyr m^{-1} at NP. At 1.5 Ma, it is between 9 and 12 kyr m^{-1}.

https://doi.org/10.5194/egusphere-2023-157
Preprint. Discussion started: 23 February 2023

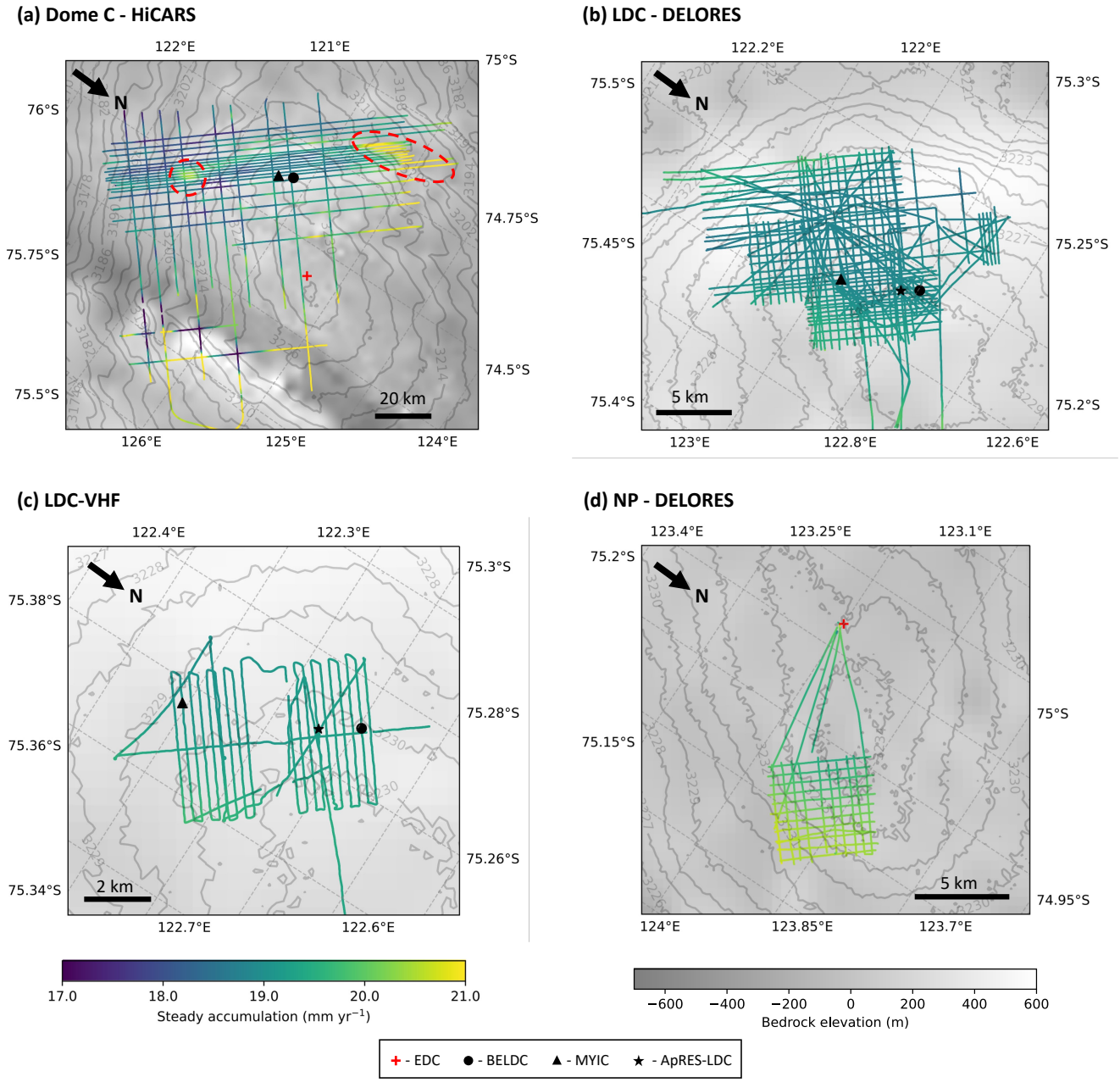

Figure 7. Modelled temporally averaged ice-equivalent surface accumulation rate for each study. Colour bars correspond to all four panels. **(a)** HiCARS airborne dataset, red dashed circles show local depressions in the bedrock which have higher accumulation rates than surrounding areas. **(b)** LDC DELORES ground based radar, **(c)** LDC-VHF high resolution ground based radar dataset, **(d)** NP DELORES dataset.

https://doi.org/10.5194/egusphere-2023-157
Preprint. Discussion started: 23 February 2023

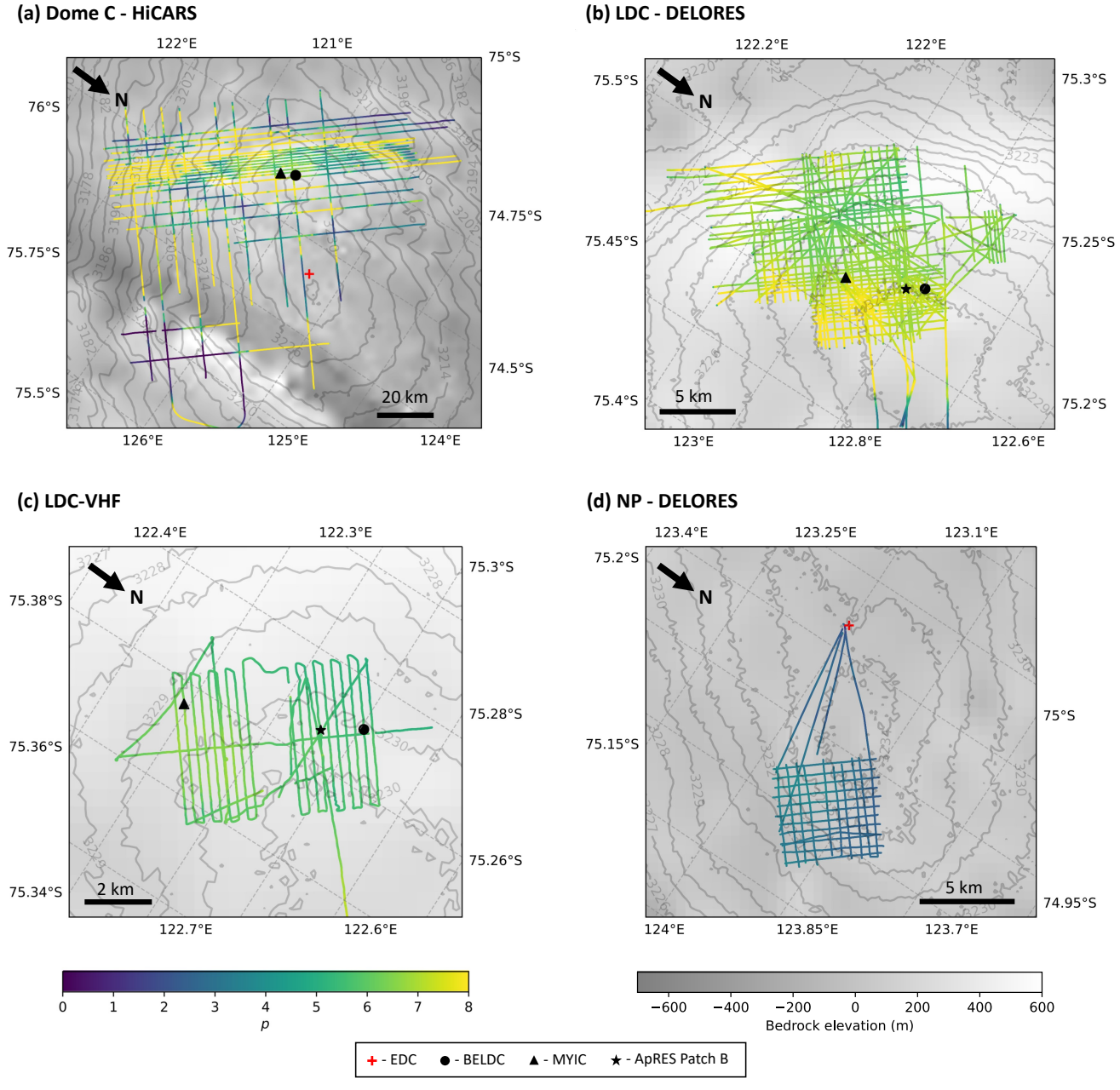

Figure 8. Lliboutry profile p parameter, colour bars correspond to all four panels. **(a)** HiCARS airborne dataset, **(b)** LDC DELORES ground based radar, **(c)** LDC-VHF high resolution ground based radar dataset, **(d)** NP DELORES dataset.

https://doi.org/10.5194/egusphere-2023-157
Preprint. Discussion started: 23 February 2023

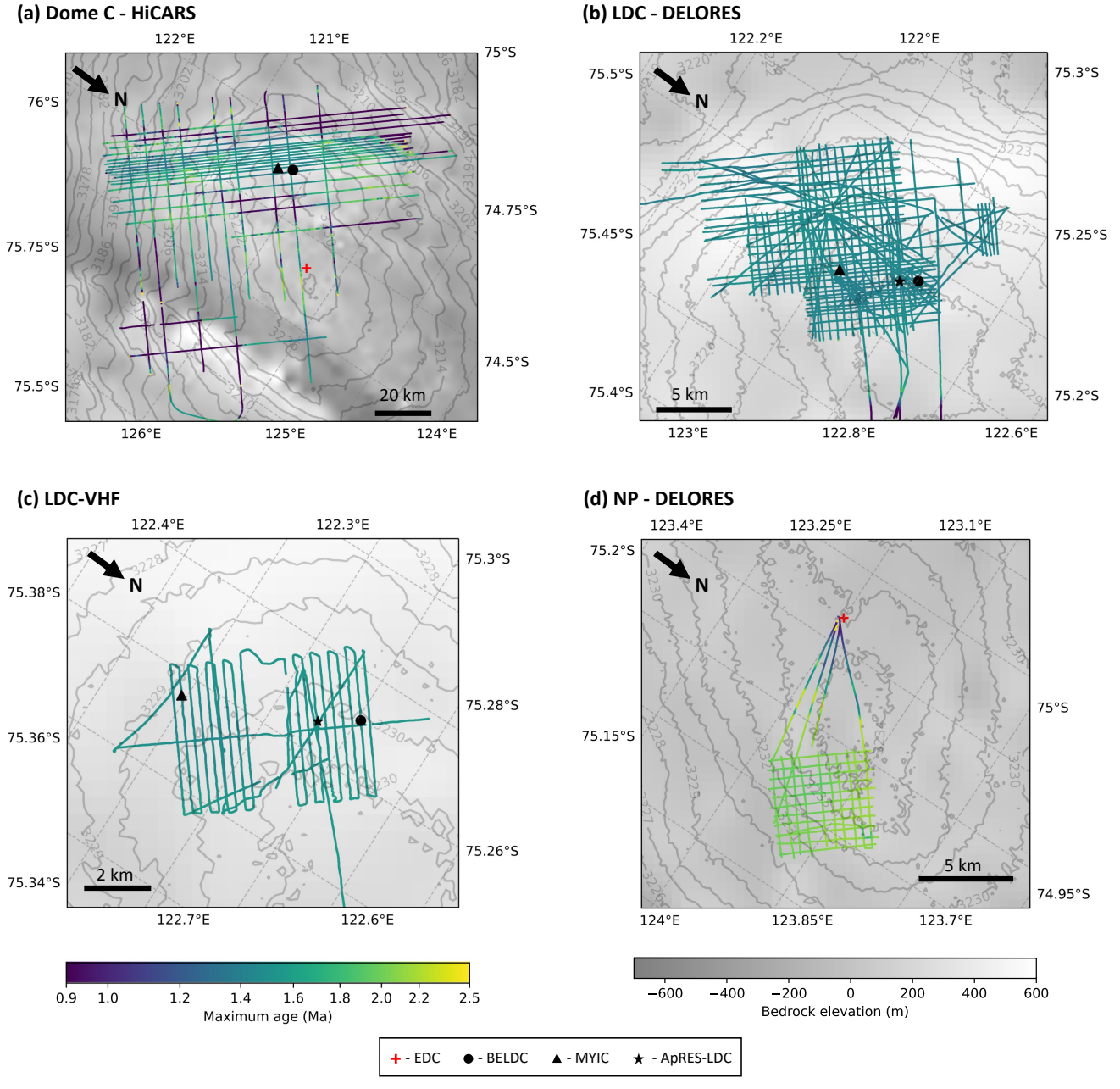

Figure 9. Maximum age with a maximum acceptable age density of 20 kyr m^{-1}, colour bars correspond to all four panels. **(a)** HiCARS airborne dataset, **(b)** LDC DELORES ground based radar, **(c)** LDC-VHF high resolution ground based radar dataset, **(d)** NP DELORES dataset.

https://doi.org/10.5194/egusphere-2023-157
Preprint. Discussion started: 23 February 2023

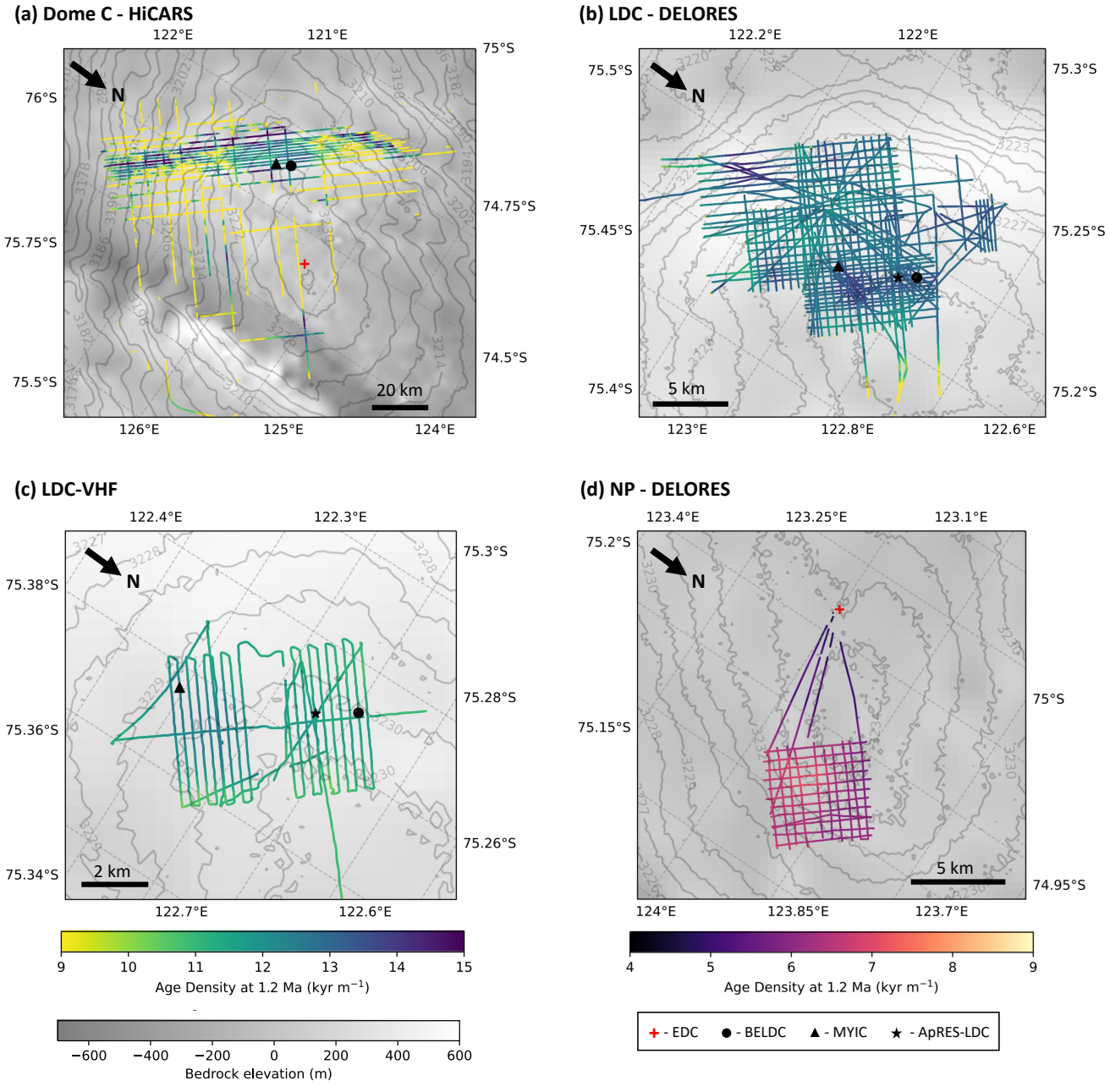

Figure 10. Age density at 1.2 Ma, the left hand colour bar corresponds to maps (a-c), the right hand colour bar corresponds to (d) and the bedrock elevation colour bar corresponds to all four panels. **(a)** HiCARS airborne dataset, **(b)** LDC DELORES ground based radar, **(c)** LDC-VHF high resolution ground based radar dataset, **(d)** NP DELORES dataset.

https://doi.org/10.5194/egusphere-2023-157
Preprint. Discussion started: 23 February 2023

4.6 Age and age density predictions at LDC

Both the DELORES and LDC-VHF radar transects are collected very close to the new BELDC drill site, at distances of 21 m and 37 m, respectively. Therefore, using the model results, we can infer the potential properties of the core (see Table IV). The inverted mechanical ice thickness H_m is 2546±30 m and 2596±34 m for the two datasets, which gives a thickness for the stagnant ice of 210±35 m and 161±41 m, respectively. The top of the basal unit was traced 154 m above the bedrock in this study, and Lilien et al. (2021) gave a basal unit thickness of ∼200 m for the same radar line.

	BELDC		MYIC	
	DELORES HRB7-HRB8	LDC-VHF 20201004	DELORES BV34B-BV34E-2	LDC-VHF 20201009
Distance of closest point to drill site (m)	21	37	55	0.5
Total ice thickness H_{obs} (m)	2756	2757	2758	2742
Mechanical ice thickness H_m (m)	2546±30	2596±34	2555±25	2576±34
Stagnant ice thickness (m)	210±35	161±41	202±35	165±42
Depth of 1.2 Ma ice (m)	2469	2503	2477	2492
Age density at 1.2 Ma (kyr m^{-1})	13.2	11.2	13.0	12.2
Depth of 1.5 Ma ice (m)	2487	2523	2495	2511
Maximum age at 20 kyr m^{-1} (Ma)	1.43±0.16	1.54±0.18	1.43±0.17	1.49±0.19
Depth of max age ice (m)	2484	2526	2492	2504

Table IV. Modelling results for the BELDC and MYIC drill sites.

At BELDC, the maximum ages at 20 kyr m^{-1} are 1.43±0.16 Ma at 2484 m from the DELORES dataset and 1.54±0.18 at 2526 m for the LDC-VHF dataset. Below the depth of this maximum age and above the stagnant ice, the remaining ice thickness is 62 m and 21 m, respectively. Potentially, this older ice could still be useful for paleoclimatic studies, if it is not too folded or disturbed. The age density of 1.2 Ma ice is 13.2 kyr m^{-1} at a depth of 2469 m and 11.2 kyr m^{-1} at a depth of 2503 m, respectively.

Figure 11 shows the age profiles at BELDC from our two radar datasets, with the Lilien et al. (2021) results for comparison. The points and horizontal bars represent the isochrones and uncertainties from Tables I (DELORES, orange) and II (LDC-VHF, blue) are also displayed as horizontal bars. The orange and blue curves show the modelled ages, with their uncertainties in the corresponding shaded colour. We also show the observed bedrock depths (H_{obs} from Table IV), the depths of the top of the stagnant ice (H_m) and the observed top of the basal unit from the LDC-VHF dataset.

Table IV also shows the model results for the MYIC drill site. With the exception of total ice thickness H_{obs}, this site shows more consistent values between the DELORES and LDC-VHF datasets than are calculated at BELDC. The average values for all characteristics highlighted are within uncertainties for the two drill sites. An analagous age-depth profile figure for MYIC can be found in the Supplementry material (Fig S1).

https://doi.org/10.5194/egusphere-2023-157
Preprint. Discussion started: 23 February 2023

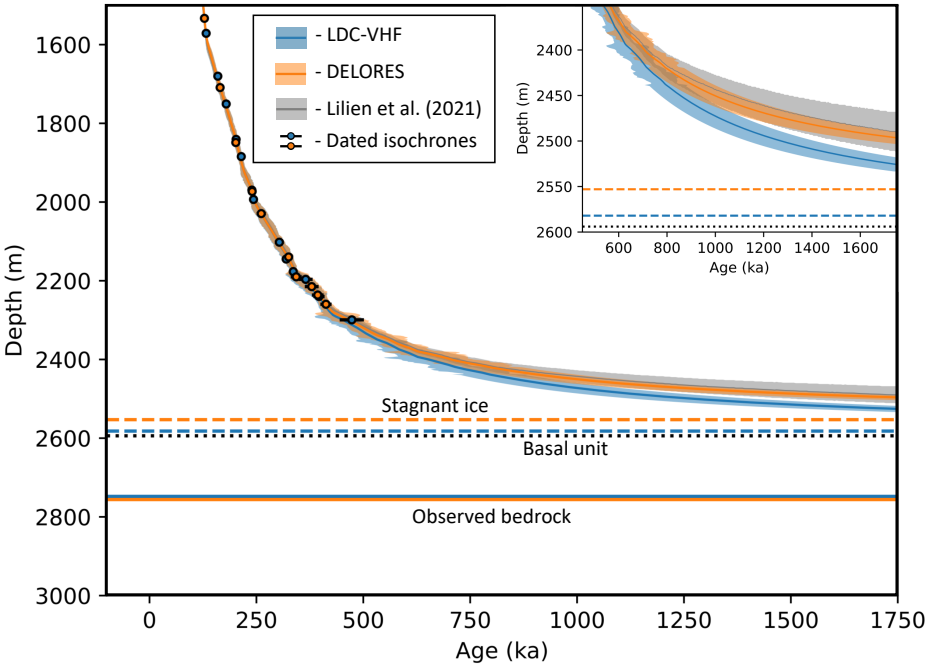

Figure 11. Modelled age depth profile at the BELDC drill site along with age uncertainty. Results for the DELORES dataset are in orange, results for the LDC-VHF dataset are in blue with the shaded areas showing 1σ uncertainty. Black circles are the isochrone ages with their age uncertainties shown as horizontal bars (Tables I and II respectively). The thick continuous lines show the radar observed bedrock depths H_{obs} (colors indicating the dataset origin), the dashed lines provide the top of the modelled stagnant ice layer H_m and the dotted black line shows the top of the basal unit traced in the LDC-VHF radar survey. The inset shows the deepest modelled section in more detail. Grey shows the result and 1σ uncertainty from modelling in Lilien et al. (2021) using isochrones continuously traced from BELDC to EDC.

5 Discussion

5.1 Modelling limitations

In this section, we discuss the limitations when using a 1D numerical model. The pseudo-steady assumption means that the ratio between accumulation and melting is constant in time. The temporal accumulation variation $r(t)$ is calculated directly from AICC2012 (Bazin et al., 2013) so it is assumed to be identical to that inferred from the EDC ice core for all radar datasets. Of the available ice core records, EDC provides the most suitable accumulation record for the LDC and NP sites as its proximity implies that it shares similar local conditions. Moreover, unlike the Vostok ice core for example, where there is significant horizontal flow so deeper ice originates from further upstream than the shallower ice, EDC is relatively unaffected by local factors. EDC is ∼35 km from LDC and ∼10 km from NP, so the accumulation rates are unlikely to be drastically different (Le Meur et al., 2018). The oldest ice found at EDC was 800 ka, therefore information on the accumulation variation $r(t)$ is limited to ice younger than this. If accumulation rates were higher before the MPT then the model would under-estimate

https://doi.org/10.5194/egusphere-2023-157
Preprint. Discussion started: 23 February 2023

layer thickness and therefore the age of the ice would be over-estimated. A possible solution could be to infer accumulation variations from marine sediment cores (Lisiecki and Raymo, 2005) for ice over 800 ka. The model does not account for any ice thickness variation over time, though this might only affect the thinning function by a few percent (Parrenin et al., 2007). The truncation of the vertical velocity profile implies basal sliding can be present when there is basal melting but it is not calculated independently. Figure 10 shows that the p parameter is higher at LDC than at NP. There are a few possible explanations for this. It could be due to the relatively thick layer of stagnant ice at LDC, which could smooth the bedrock roughness making basal sliding more likely. Around the edges of LDC, p is even higher suggesting that basal sliding is greater further from the divide. The Raymond effect (Raymond, 1983) could also be a contributing factor, making p larger away from the dome. Ice may come from upstream where the glaciological conditions are different, such as different ice thickness, therefore, variations of p could be an artifact of the 1D assumption. Parrenin et al. (2017) also found this trend, though their p values are generally lower than those modelled in this study especially near the LDC area. This is likely due to the addition of the variable mechanical ice thickness. It allows a layer of stagnant ice to exist which is not included in the thinning function below the mechanical ice depth. This means that the thinning function is more linear giving a greater p value for our model.

Passalacqua et al. (2017) inferred basal melt rates using a model that incorporated geothermal heat flux, unlike in this study. They found similar results such as no melting across the LDC bedrock relief (Fig. 3). Around the edges of LDC and in the Concordia trench, we infer a melt rate that agrees with the trend suggested by Passalacqua et al. (2017). In Sect. 4.1, we showed the results for EDC in order to evaluate the model as we had observations to compare to. At EDC, the modelled melt rate was around 0.34 mm yr^{-1}, which agrees with the suggested presence of melt water found in the seismic sounding of the drill hole and Passalacqua et al. (2017), who found the melt rate to be around 0.3 mm yr^{-1}. This is lower than the previous modelled result of 0.56$\pm$0.19 mm yr^{-1} from Parrenin et al. (2007). At the deepest dated point on the EDC ice core (3189 m), we found a modelled age (Table IV) around 100-200 kyr older than would be expected from the AICC2012 age-depth profile (801$\pm$96 ka, Bazin et al., 2013). The shape of the thinning function means that the age scale increases exponentially to infinity as the mechanical thickness H_m is reached. Looking at the AICC2012 EDC profile determined from experimental measurements, it follows an exponential profile until the lower 200 m of dated ice, perhaps meaning that the thinning is for some reason lower than the model would expect. This effect was also observed by Obase et al. (2022, see Fig. 6 of that publication) at Dome Fuji, who used the Lliboutry vertical velocity profile (Eq. 3) in a transient 1D model. They found that the AICC2012 chronology begins to deviate from their exponential modelled age-depth profile at around 300 m above the bed at Dome Fuji, where the true age is then significantly younger than the modelled one. This could mean our age predictions for BELDC are over-estimated at depths up to 300 m above the bed where the relationship becomes less exponential. Further uncertainty is added when considering the 182$\pm$63 m modelled stagnant ice thickness at BELDC, and whether it can be included in this area of reduced thinning at the base of the ice sheet.

The 1D nature of this model means that effects due to horizontal flow are not considered. Along the Dome C divide, this is a reasonable assumption. However, where ice flows along the Concordia trench as seen in the HiCARS radar dataset, the model becomes less stable. Figure 12 shows that the reliability index (Eq. 5) is less than 2 in most of the surveyed area and even less than 1 over LDC and NP, therefore our assumptions seem to be well adapted.

https://doi.org/10.5194/egusphere-2023-157
Preprint. Discussion started: 23 February 2023

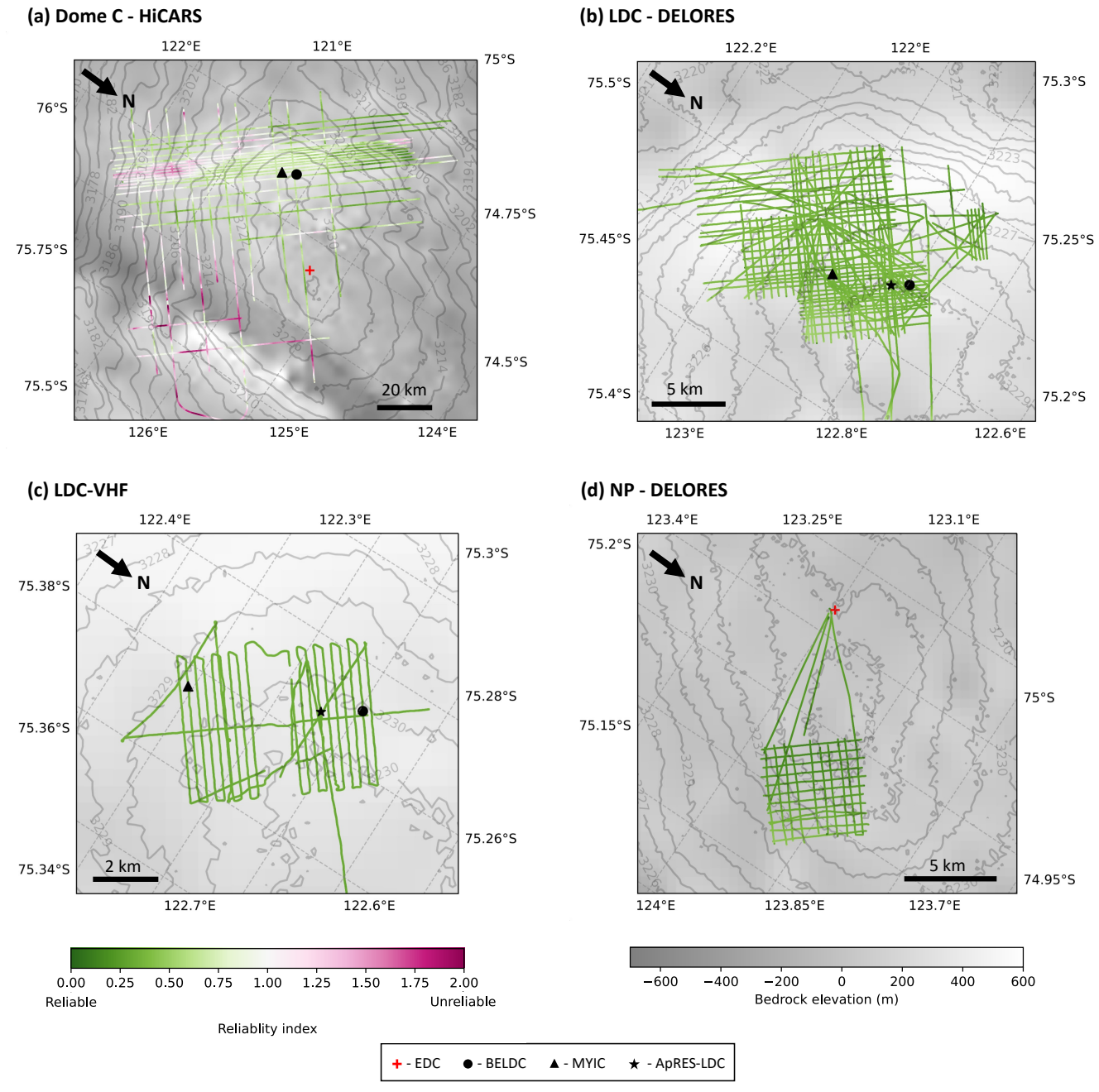

Figure 12. Reliability of the model, from 0 green (reliable) to 2 dark pink (unreliable), both colour bars correspond to all four panels. **(a)** HiCARS airborne dataset, **(b)** LDC DELORES ground based radar, **(c)** LDC-VHF high resolution ground based radar dataset, **(d)** NP DELORES dataset.

https://doi.org/10.5194/egusphere-2023-157
Preprint. Discussion started: 23 February 2023

In order to account for horizontal flow, we suggest that a 2.5D model would be most appropriate, a pseudo-steady geometry could be maintained as a lagrangian/semi-lagrangian tracer scheme would not be required. Sutter et al. (2021) showed that it is possible to use a non-pseudo-steady model, though it is more challenging as it requires more detailed knowledge of boundary conditions and temporal accumulation variations. Currently the spatial resolution for this type of model is also too low relative to the scales of the processes discussed here, when taking into account small scale bedrock relief and high spatial radar resolution, for example.

5.2 Radar dataset limitations

In Sect. 4.1, we look at the radar data sites that pass the closest to EDC, which includes four DELORES transects and one LDC-VHF transect. The most accurate estimate of the ice thickness at EDC is 3273±5 m (Parrenin et al., 2007), determined using the length of the core and the drilling cable, and accounting for hole inclination. In this study, the total ice thicknesses in Table III come directly from the bedrock interface traced in each radar dataset and agree well with Lilien et al. (2021) who independently traced the bedrock depth in the LDC-VHF dataset as 3238 m. They suggested that the difference between the radar measured bedrock return and the drill hole bottom measured could be due to factors such as "off-nadir reflection, debris in the ice, small differences in topography over the 178 m offset, and uncertainty in firn-air content and wave speed". The DELORES dataset is also shallower than expected probably for similar reasons.

The depth distribution of the IRHs traced in each dataset is quite different. Both the HiCARS and DELORES datasets have dated IRHs from ∼10 ka (∼300 m depth). Whereas for the LDC-VHF dataset, it was only possible to trace IRHs below 1000 m because of the length of the transmission chirp (8 µs), which blanks the upper parts of the ice sheet such that the first observable isochrone is much older (73.3 ka). The age of the oldest date-able IRH is limited by the radar transect linking LDC to the EDC ice core for dating. The basal melting along the divide between EDC and LDC (Fig 3a) means that deep IRHs are either discontinuous or completely melted in some places. Therefore, IRHs over 500 ka can only be discontinuously traced from LDC to EDC, as done by Lilien et al. (2021). In this study, the same method was used to trace four further discontinuous IRHs in the DELORES radar data however, the uncertainty was too high for them to be considered here. Cavitte et al. (2021) traced seven deep IRHs in the HiCARS dataset which could not be linked to EDC. They used a different numerical model to date the IRHs and found that at LDC, their oldest IRH was ∼700 ka. A new age depth profile from an ice core at LDC, such as at BELDC or MYIC, would mean that deeper IRHs could be continuously traced to an ice core record for dating. Having deeper dated IRHs would help to constrain the model at lower depths giving a more accurate thinnning function and would therefore yield more accurate model results for the whole LDC area.

The ability to observe the internal structure of the basal unit in the radar data is relatively new (Lilien et al., 2021; Cavitte, 2017), as previously radar systems did not have sufficiently high vertical resolution. As a result no tracing convention has yet been established, so the identification of the top of the basal unit depends strongly on the chosen convention of the human tracer, which may explain the differences between this study and that of Lilien et al. (2021). Further work should be done to establish a standard procedure for the treatment of internal layers, as for instance considered by the SCAR Action Group AntArchitecture (AntArchitecture Steering Committee) for tracing the basal unit in radargrams.

https://doi.org/10.5194/egusphere-2023-157
Preprint. Discussion started: 23 February 2023

5.3 Nature of the stagnant unit

Tison et al. (2015) found that the paleoclimatic signal from the ice in the bottom 60 m of the EDC ice core was not clear and the time scale distorted. They suggested that since this deepest ice was almost at melting point, there could be a mechanism of chemical sorting acting on the impurities. Bell et al. (2011) presented radargrams which they interpreted as refrozen ice at the base of the Dome A ice sheet. The appearance in the radar data of the basal unit at Dome C is very different to Dome A, as layer fragments are visible. However, ice with entrapment of basal debris, partly containing refrozen ice (e.g. from regelation in the past) cannot be ruled out as a source of stagnant ice as it could be that the Dome A radar system was not able to pick up weaker, fragmented signals. The upper part of the EFZ observed by Drews et al. (2009) at EDML seems to have been a signature of the radar, related to sub-resolution changes in physical properties, as the Ruth et al. (2007) analysis of the ice core showed that a paleoclimatic signal could be found in the top half of the EFZ. The basal unit observed in the LDC-VHF data of this study and published in Lilien et al. (2021) is different because the radar system is sufficiently sensitive at this depth, so the effect is likely to come from physical changes in the ice. The ApRES measurements at LDC show that the ice at the depth of the basal unit has different properties to that above. Moreover, the ApRES-LDC vertical velocity (Fig 6a) increases to zero more quickly than at EDC (Fig 6b) at similar normalised depths. It follows from the ApRES-LDC measurements that there is almost no deformation in the basal ice so it must be nearly or totally stagnant. Our model effectively shows that in order to better fit the isochrones, the vertical strain-rates near the surface must be higher over LDC than would be produced by a profile which follows the Lliboutry (1979) variation over the full depth.

In Sect. 4.3 we showed that the thicknesses of the modelled stagnant ice and the observed basal unit are comparable and have similar shapes. The ApRES results also showed that the best fit for the vertical velocity profile occurs when we include a layer of stagnant basal ice. Therefore our results are compatible with the hypothesis that this basal unit observed by the LDC-VHF radar system is indeed stagnant. It appears that irregularities, such as local dips, in the bedrock are filled in by the basal layer. The isochrones therefore follow the smooth shape of the top of the basal layer, which could have implications for the overall ice sheet dynamics. For example, if the ice sheet is sliding above the basal unit, it could smooth the roughness and decrease basal drag. This would in turn increase the horizontal flux. However, the thickness of the flowing ice decreases which would reduce the total horizontal flux. In order to quantify which of these mechanisms has a larger effect, flow modelling in different areas of Antarctica would be required. There are many unanswered questions regarding the basal layer. It is unknown if the basal layer exists elsewhere in Antarctica and if so, how much of the ice sheet it covers. If it is widespread, it could influence future sea level estimates by decreasing the basal drag.

The ice core to be extracted at BELDC could yield a basal layer of almost 200 m. Analysing its fabric structure, age, air composition, isotopic composition and impurities will substantially advance our understanding of the basal layer found around Dome C.

https://doi.org/10.5194/egusphere-2023-157
Preprint. Discussion started: 23 February 2023

5.4 Oldest Ice prospects

We confirm that the BELDC site is promising for retrieving ice old enough to study the MPT. Our results for BELDC are compatible with those of Lilien et al. (2021), who found that the 1.5 Ma isochrone is at 2498±14 m depth at BELDC with an age density of 19±2 kyr m^{-1}. Our results therefore confirm that, despite the stagnant ice present in the bottom of the ice sheet, the BELDC drilling site should reach its target of 1.5 Ma, although it might be at the limit in terms of acceptable age density. A safer expectation for Oldest Ice is 1.2 Ma, as the modelled age density is 12.2 kyr m^{-1}, which is well within the 20 kyr m^{-1} target (Fischer et al., 2013). Also, it should still cover the MPT and the last part of the 40-kyr world. The MYIC site has very similar characteristics to BELDC. The differences between the two ice cores could help inform future site prospecting as they may show evidence of processes that are not detectable from the radar data or have not been considered in the model.

We also investigated NP as a potential area for finding old ice. According to the model, age density at 1.5 Ma is twice as good as that of LDC. This is due to the relative lack of stagnant ice predicted by the model at NP, which at LDC causes more thinning of the deepest ice. The reason that NP was not considered further for the Beyond EPICA project was that basal melting at LDC was much less likely, making it the safer option. While the NP was initally flagged by a HiCARS transect passing nearby, the only detailed radar data available at NP are the DELORES transects. In order to determine the suitability of NP as an Oldest Ice site, it would be useful to conduct a radar survey using the multichannel coherent radar depth sounders like LDC-VHF. The methodology implemented in this study can be applied to other areas of Antarctica in the search for Oldest Ice such as Dome A, Dome B, Dome Fuji (Wang et al., companion paper) etc.

6 Conclusions

In this paper, we presented a 1D numerical model which interpolates and extrapolates the age–depth profile while being constrained by traced and dated radar IRHs. The model was applied to three datasets collected over the LDC area and the model outputs show similar results regarding the stagnant ice thickness and maximum age in the lowest part of the ice. The model was validated by comparing the results with the EDC ice core record. It was shown that the thickness of the modelled stagnant ice is comparable to that of the basal unit observed in the radar, supporting the hypothesis that this basal unit is stagnant. ApRES measurements at EDC and LDC also showed that the vertical velocity profile can be best explained when a basal layer of stagnant ice is present. The maximum modelled age at 20 kyr m^{-1} for the transect location closest to the BELDC drill site is 1.49±0.18 Ma at 2505±34 m depth. The resolution of 1.2 Ma old ice is 12.2 kyr m^{-1} at a depth of 2486±34 m. The predicted thickness of stagnant ice at the base of the ice sheet is 182±63 m. The MYIC site on LDC also yields similar modelled results. The model was also applied to NP near Dome C where the maximum age was around 2 Ma and age density of 1.5 Ma ice was around twice as good as that found at the LDC drill sites, making it a potentially promising site for future Oldest Ice projects. The 1D model can be applied to any other area that is close to a divide so that horizontal flow is negligible. The development of a more complex 2.5D model which takes into account the horizontal flow of an ice sheet will allow us to look for old ice in other areas of Antarctica, especially with the collection of new more spatially extensive and denser radar campaigns.

https://doi.org/10.5194/egusphere-2023-157
Preprint. Discussion started: 23 February 2023

Code availability. The code for the 1D numerical model is availible publically from https://github.com/ailsachung/IsoInv1D

Data availability. The HiCARS IRHs used in this study can be found publicly on the US Antarctic Program Data Center (USAP-DC): https://doi.org/10.15784/601411 (Cavitte et al., 2020). The DELORES profiles discussed in this paper will be available from https://data.bas.ac.uk. LDC-VHF radar will be made publically available in a PANGAEA repository. DELORES and LDC-VHF IRHs used in this study will be publically available in a PANGAEA repository. Bedmachine version 3 bed elevation data comes from the work of Morlighem et al. (2020) and is available on https://nsidc.org/data/NSIDC-0756/versions/3 (date accessed: 25 Jan 23). REMA surface elevation data is from the work of Howat et al. (2019) available on https://www.pgc.umn.edu/data/rema/.

Author contributions. AC traced radar isochrones in the DELORES and LDC-VHF datasets with help from by RM, DS and OE. AC also improved on model developed by FP, and ran experiments with supervision from FP and OE. DS, RM, DT, DL, VH, CR, CM, CO, MF, PG, HM, DDJ and OE were involved in DELORES and LDC-VHF radar survey design, data acquisition and processing. AC prepared the manuscript with relevant input from all co-authors.

Competing interests. CM & OE are editors of The Cryosphere and OE is coordinator of the inter-journal SI. The authors declare no other competing interests.

Acknowledgements. This publication was generated in the frame of Beyond EPICA. The project has received funding from the European Union's Horizon 2020 research and innovation programme under grant agreement No. 815384 (Oldest Ice Core). It is supported by national partners and funding agencies in Belgium, Denmark, France, Germany, Italy, Norway, Sweden, Switzerland, The Netherlands and the United Kingdom. Logistic support is mainly provided by ENEA and IPEV through the Concordia Station system. This publication was generated in the frame of DEEPICE project. The project has received funding from the European Union's Horizon 2020 research and innovation programme under the Marie Sklodowska-Curie grant agreement No 955750. AWI acknowledges Pascal Andreas and Sven Lenius for their contribution to the preprocessing of the data.

The opinions expressed and arguments employed herein do not necessarily reflect the official views of the European Union funding agency or other national funding bodies. This is Beyond EPICA publication number XX.

https://doi.org/10.5194/egusphere-2023-157
Preprint. Discussion started: 23 February 2023

References

AntArchitecture Steering Committee: AntArchitecture, https://www.scar.org/science/antarchitecture/.

Bazin, L., Landais, A., Lemieux-Dudon, B., Toyé Mahamadou Kele, H., Veres, D., Parrenin, F., Martinerie, P., Ritz, C., Capron, E., Lipenkov, V., Loutre, M. F., Raynaud, D., Vinther, B., Svensson, A., Rasmussen, S. O., Severi, M., Blunier, T., Leuenberger, M., Fischer, H., Masson-Delmotte, V., Chappellaz, J., and Wolff, E.: An optimized multi-proxy, multi-site Antarctic ice and gas orbital chronology (AICC2012): 120-800 ka, Climate of the Past, 9, 1715–1731, https://doi.org/10.5194/cp-9-1715-2013, 2013.

Bell, R. E., Ferraccioli, F., Creyts, T. T., Braaten, D., Corr, H., Das, I., Damaske, D., Frearson, N., Jordan, T., Rose, K., Studinger, M., and Wolovick, M.: Widespread persistent thickening of the east antarctic ice sheet by freezing from the base, Science, 331, 1592–1595, https://doi.org/10.1126/science.1200109, 2011.

Buizert, C., Fudge, T. J., Roberts, W. H. G., Steig, E. J., Sherriff-Tadano, S., Ritz, C., Lefebvre, E., Edwards, J., Kawamura, K., Oyabu, I., Motoyama, H., Kahle, E. C., Jones, T. R., Abe-Ouchi, A., Obase, T., Martin, C., Corr, H., Severinghaus, J. P., Beaudette, R., Epifanio, J. A., Brook, E. J., Martin, K., Chappellaz, J., Aoki, S., Nakazawa, T., Sowers, T. A., Alley, R. B., Ahn, J., Sigl, M., Severi, M., Dunbar, N. W., Svensson, A., Fegyveresi, J. M., He, C., Liu, Z., Zhu, J., Otto-Bliesner, B. L., Lipenkov, V. Y., Kageyama, M., and Schwander, J.: Antarctic surface temperature and elevation during the Last Glacial Maximum, Science, 372, 1097–1101, https://doi.org/10.1126/science.abd2897, 2021.

Cavitte, M., Young, D., Mulvaney, R., Ritz, C., Greenbaum, J., Ng, G., Kempf, S., Quartini, E., Muldoon, G., Paden, J., Frezzotti, M., Roberts, J., Tozer, C., Schroeder, D., and Blankenship, D.: A detailed radiostratigraphic data set for the central East Antarctic Plateau spanning the last half million years, Earth System Science Data Discussions, pp. 1–27, https://doi.org/10.5194/essd-2020-393, 2021.

Cavitte, M. G., Blankenship, D. D., Young, D. A., Schroeder, D. M., Parrenin, F., Lemeur, E., MacGregor, J. A., and Siegert, M. J.: Deep radiostratigraphy of the East Antarctic plateau: Connecting the Dome C and Vostok ice core sites, Journal of Glaciology, 62, 323–334, https://doi.org/10.1017/jog.2016.11, 2016.

Cavitte, M. G., Parrenin, F., Ritz, C., Young, A., Van Liefferinge, B., Blankenship, D. D., Frezzotti, M., and Roberts, J. L.: Accumulation patterns around Dome C, East Antarctica, in the last 73 kyr, Cryosphere, 12, 1401–1414, https://doi.org/10.5194/tc-12-1401-2018, 2018.

Cavitte, M. G. P.: Flow Re-Organization of the East Antarctic Ice Sheet Across Glacial Cycles, Ph.D. thesis, The University of Texas at Austin, 2017.

Cavitte, M. G. P., Young, D. A., Mulvaney, R., Ritz, C., Greenbaum, J., Ng, G., Kempf, S. D., Quartini, E., Muldoon, G. R., Paden, J., Frezzotti, M., Roberts, J., Tozer, C., Schroeder, D., and Blankenship, D. D.: "Ice-penetrating radar internal stratigraphy over Dome C and the wider East Antarctic Plateau" U.S. Antarctic Program (USAP) Data Center., https://doi.org/10.15784/601411, 2020.

Clark, P. U., Archer, D., Pollard, D., Blum, J. D., Rial, J. A., Brovkin, V., Mix, A. C., Pisias, N. G., and Roy, M.: The middle Pleistocene transition: characteristics, mechanisms, and implications for long-term changes in atmospheric pCO2, Quaternary Science Reviews, 25, 3150–3184, https://doi.org/10.1016/j.quascirev.2006.07.008, 2006.

Drews, R., Eisen, O., Weikusat, I., Kipfstuhl, S., Lambrecht, A., Steinhage, D., Wilhelms, F., and Miller, H.: Layer disturbances and the radio-echo free zone in ice sheets, Cryosphere, 3, 195–203, https://doi.org/10.5194/tc-3-195-2009, 2009.

EPICA members: Eight glacial cycles from an Antarctic ice core, Nature, 429, 623–628, https://doi.org/10.1038/nature02599, 2004.

Fischer, H., Severinghaus, J., Brook, E., Wolff, E., Albert, M., Alemany, O., Arthern, R., Bentley, C., Blankenship, D., Chappellaz, J., Creyts, T., Dahl-Jensen, D., Dinn, M., Frezzotti, M., Fujita, S., Gallee, H., Hindmarsh, R., Hudspeth, D., Jugie, G., Kawamura, K., Lipenkov, V., Miller, H., Mulvaney, R., Parrenin, F., Pattyn, F., Ritz, C., Schwander, J., Steinhage, D., Van Ommen, T., and Wilhelms, F.: Where to

https://doi.org/10.5194/egusphere-2023-157
Preprint. Discussion started: 23 February 2023

find 1.5 million yr old ice for the IPICS "Oldest-Ice" ice core, Climate of the Past, 9, 2489–2505, https://doi.org/10.5194/cp-9-2489-2013, 2013.

Howat, I. M., Porter, C., Smith, B. E., Noh, M. J., and Morin, P.: The reference elevation model of antarctica, Cryosphere, 13, 665–674, https://doi.org/10.5194/tc-13-665-2019, 2019.

Kingslake, J., Martín, C., Arthern, R. J., Corr, H. F., and King, E. C.: Ice-flow reorganization in West Antarctica 2.5 kyr ago dated using radar-derived englacial flow velocities, Geophysical Research Letters, 43, 9103–9112, https://doi.org/10.1002/2016GL070278, 2016.

Le Meur, E., Magand, O., Arnaud, L., Fily, M., Frezzotti, M., Cavitte, M., Mulvaney, R., and Urbini, S.: Spatial and temporal distributions of surface mass balance between Concordia and Vostok stations, Antarctica, from combined radar and ice core data: First results and detailed error analysis, Cryosphere, 12, 1831–1850, https://doi.org/10.5194/tc-12-1831-2018, 2018.

Lilien, D. A., Steinhage, D., Taylor, D., Parrenin, F., Ritz, C., Mulvaney, R., Martín, C., Yan, J. B., O'Neill, C., Frezzotti, M., Miller, H., Gogineni, P., Dahl-Jensen, D., and Eisen, O.: Brief communication: New radar constraints support presence of ice older than 1.5 Myr at Little Dome C, Cryosphere, 15, 1881–1888, https://doi.org/10.5194/tc-15-1881-2021, 2021.

Lisiecki, L. E. and Raymo, M. E.: A Pliocene-Pleistocene stack of 57 globally distributed benthic δ 18O records, Paleoceanography, 20, 1–17, https://doi.org/10.1029/2004PA001071, 2005.

Livingstone, S. J., Li, Y., Rutishauser, A., Sanderson, R. J., Winter, K., Mikucki, J. A., Björnsson, H., Bowling, J. S., Chu, W., Dow, C. F., Fricker, H. A., McMillan, M., Ng, F. S., Ross, N., Siegert, M. J., Siegfried, M., and Sole, A. J.: Subglacial lakes and their changing role in a warming climate, Nature Reviews Earth and Environment, 3, 106–124, https://doi.org/10.1038/s43017-021-00246-9, 2022.

Lliboutry, L.: A critical review of analytical approximate solutions for steady state velocities and temperatures in cold ice sheets, in: Z. Gletscherkde. Glazialgeol., vol. 15, pp. 135–148, 1979.

Morlighem, M.: MEaSUREs BedMachine Antarctica, Version 3, https://doi.org/10.5067/FPSU0V1MWUB6, 2022.

Morlighem, M., Rignot, E., Binder, T., Blankenship, D., Drews, R., Eagles, G., Eisen, O., Ferraccioli, F., Forsberg, R., Fretwell, P., Goel, V., Greenbaum, J. S., Gudmundsson, H., Guo, J., Helm, V., Hofstede, C., Howat, I., Humbert, A., Jokat, W., Karlsson, N. B., Lee, W. S., Matsuoka, K., Millan, R., Mouginot, J., Paden, J., Pattyn, F., Roberts, J., Rosier, S., Ruppel, A., Seroussi, H., Smith, E. C., Steinhage, D., Sun, B., Broeke, M. R. d., Ommen, T. D., Wessem, M. v., and Young, D. A.: Deep glacial troughs and stabilizing ridges unveiled beneath the margins of the Antarctic ice sheet, Nature Geoscience, 13, 132–137, https://doi.org/10.1038/s41561-019-0510-8, 2020.

Nicholls, K. W., Corr, H. F., Stewart, C. L., Lok, L. B., Brennan, P. V., and Vaughan, D. G.: Instruments and methods: A ground-based radar for measuring vertical strain rates and time-varying basal melt rates in ice sheets and shelves, Journal of Glaciology, 61, 1079–1087, https://doi.org/10.3189/2015JoG15J073, 2015.

Obase, T., Abe-ouchi, A., Saito, F., Tsutaki, S., and Fujita, S.: A one-dimensional temperature and age modeling study for selecting the drill site of the oldest ice core around Dome Fuji , Antarctica (Preprint), The Cryosphere Discuss, 2022.

Parrenin, F., Dreyfus, G., Durand, G., Fujita, S., Gagliardini, O., Gillet, F., Jouze, J., Kawamura, K., Lhomme, N., Masson-Delmotte, V., Ritz, C., Schwander, J., Shoji, H., Uemura, R., Watanabe, O., and Yoshida, N.: 1-D-ice flow modelling at EPICA Dome C and Dome Fuji, East Antarctica, Climate of the Past, 3, 243–259, https://doi.org/10.5194/cp-3-243-2007, 2007.

Parrenin, F., Cavitte, M. G., Blankenship, D. D., Chappellaz, J., Fischer, H., Gagliardini, O., Masson-Delmotte, V., Passalacqua, O., Ritz, C., Roberts, J., Siegert, M. J., and Young, D. A.: Is there 1.5-million-year-old ice near Dome C, Antarctica?, Cryosphere, 11, 2427–2437, https://doi.org/10.5194/tc-11-2427-2017, 2017.

Passalacqua, O., Ritz, C., Parrenin, F., Urbini, S., and Frezzotti, M.: Geothermal flux and basal melt rate in the Dome C region inferred from radar reflectivity and heat modelling, Cryosphere, 11, 2231–2246, https://doi.org/10.5194/tc-11-2231-2017, 2017.

https://doi.org/10.5194/egusphere-2023-157
Preprint. Discussion started: 23 February 2023

Raymond, C. F.: Deformation in the Vicinity of Ice Divides, Journal of Glaciology, 29, 357–373, https://doi.org/10.3189/s0022143000030288, 1983.

Ruth, U., Barnola, J. M., Beer, J., Bigler, M., Blunier, T., Castellano, E., Fischer, H., Fundel, F., Huybrechts, P., Kaufmann, P., Kipfstuhl, S., Lambrecht, A., Morganti, A., Oerter, H., Parrenin, F., Rybak, O., Severi, M., Udisti, R., Wilhelms, F., and Wolff, E.: "EDML1": A chronology for the EPICA deep ice core from Dronning Maud Land, Antarctica, over the last 150 000 years, Climate of the Past, 3, 475–484, https://doi.org/10.5194/cp-3-475-2007, 2007.

Souchez, R., Petit, J. R., Jouzel, J., Simões, J., Angelis, M. D., Barkov, N., Vimeux, F., Sleewaegen, J., Lorrain, R., Souchez, R., Petit, J. R., Jouzel, J., Simões, J., and Angelis, M. D.: Highly deformed basal ice in the Vostok core , Antarctica To cite this version : HAL Id : hal-03106876, Geophysical Research Letters, 29, 2002.

Sutter, J., Fischer, H., and Eisen, O.: Investigating the internal structure of the Antarctic ice sheet: The utility of isochrones for spatiotemporal ice-sheet model calibration, Cryosphere, 15, 3839–3860, https://doi.org/10.5194/tc-15-3839-2021, 2021.

Tison, J. L., De Angelis, M., Littot, G., Wolff, E., Fischer, H., Hansson, M., Bigler, M., Udisti, R., Wegner, A., Jouzel, J., Stenni, B., Johnsen, S., Masson-Delmotte, V., Landais, A., Lipenkov, V., Loulergue, L., Barnola, J. M., Petit, J. R., Delmonte, B., Dreyfus, G., Dahl-Jensen, D., Durand, G., Bereiter, B., Schilt, A., Spahni, R., Pol, K., Lorrain, R., Souchez, R., and Samyn, D.: Retrieving the paleoclimatic signal from the deeper part of the EPICA Dome C ice core, The Cryosphere, 9, 1633–1648, https://doi.org/10.5194/tc-9-1633-2015, 2015.

Van Liefferinge, B. and Pattyn, F.: Using ice-flow models to evaluate potential sites of million year-old ice in Antarctica, Climate of the Past, 9, 2335–2345, https://doi.org/10.5194/cp-9-2335-2013, 2013.

Wang, Z., Chung, A., Steinhage, D., Parrenin, F., Freitag, J., and Eisen, O.: Mapping age and basal conditions of ice in the Dome Fuji region , Antarctica , by combining radar internal layer stratigraphy and flow modeling.

Winter, A., Steinhage, D., Arnold, E. J., Blankenship, D. D., Cavitte, M. G., Corr, H. F., Paden, J. D., Urbini, S., Young, D. A., and Eisen, O.: Comparison of measurements from different radio-echo sounding systems and synchronization with the ice core at Dome C, Antarctica, Cryosphere, 11, 653–668, https://doi.org/10.5194/tc-11-653-2017, 2017.

Yan, J. B., Li, L., Nunn, J. A., Dahl-Jensen, D., O'Neill, C., Taylor, R. A., Simpson, C. D., Wattal, S., Steinhage, D., Gogineni, P., Miller, H., and Eisen, O.: Multiangle, Frequency, and Polarization Radar Measurement of Ice Sheets, IEEE Journal of Selected Topics in Applied Earth Observations and Remote Sensing, 13, 2070–2080, https://doi.org/10.1109/JSTARS.2020.2991682, 2020.

Young, D. A., Roberts, J. L., Ritz, C., Frezzotti, M., Quartini, E., Cavitte, M. G., Tozer, C. R., Steinhage, D., Urbini, S., Corr, H. F., Van Ommen, T., and Blankenship, D. D.: High-resolution boundary conditions of an old ice target near Dome C, Antarctica, Cryosphere, 11, 1897–1911, https://doi.org/10.5194/tc-11-1897-2017, 2017.